JÜLICH
FORSCHUNGSZENTRUM

Multiscaling from the Bottom Up

From Molecules to the Nervous System

20 March 2015 | Alexander Peyser | Simulation Lab Neuroscience / Jülich Supercomputing Centre
Institute for Advanced Simulation / Forschungszentrum Jülich

Multiscaling the Nervous System

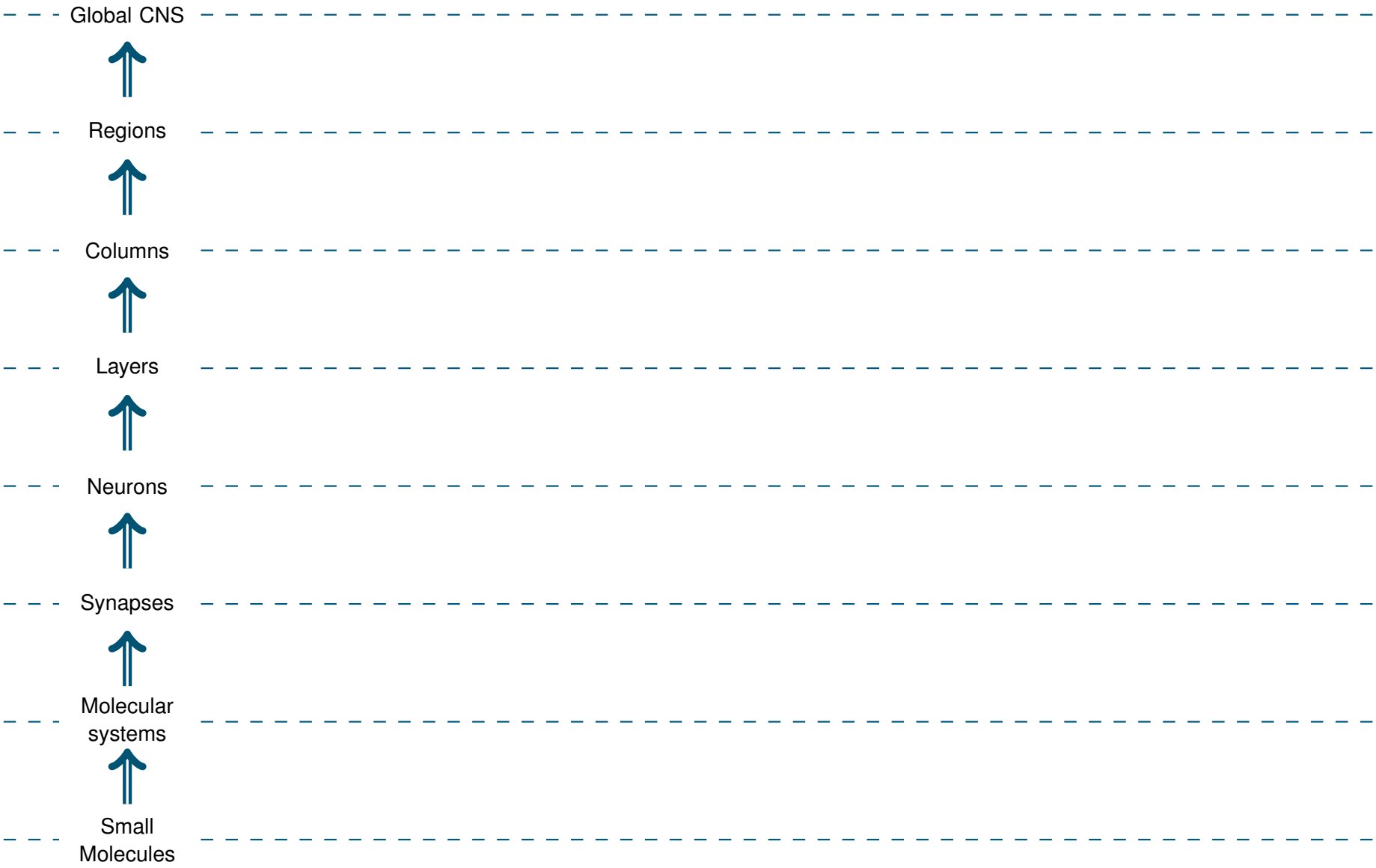

Multiscaling the Nervous System

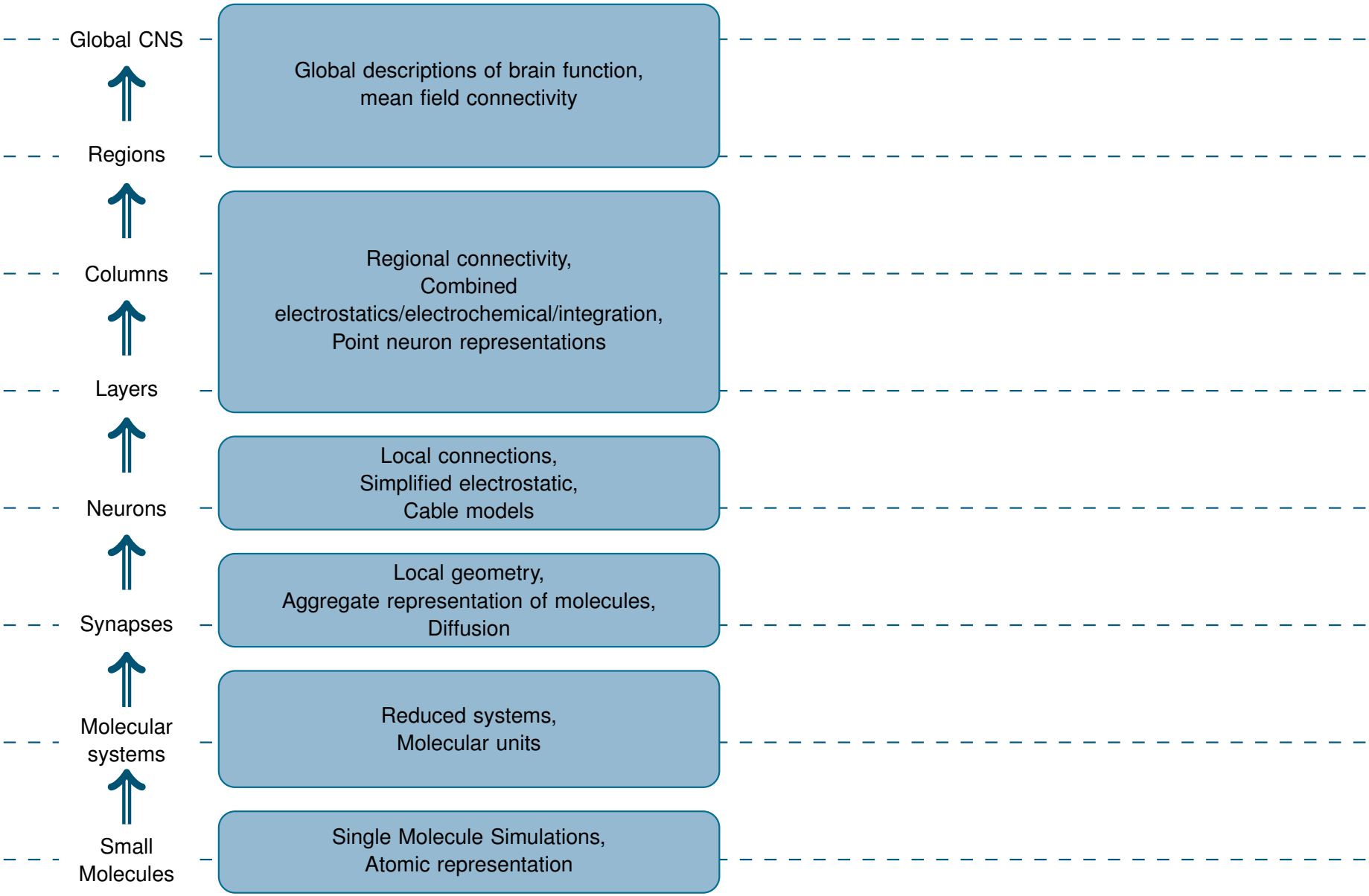

Multiscaling the Nervous System

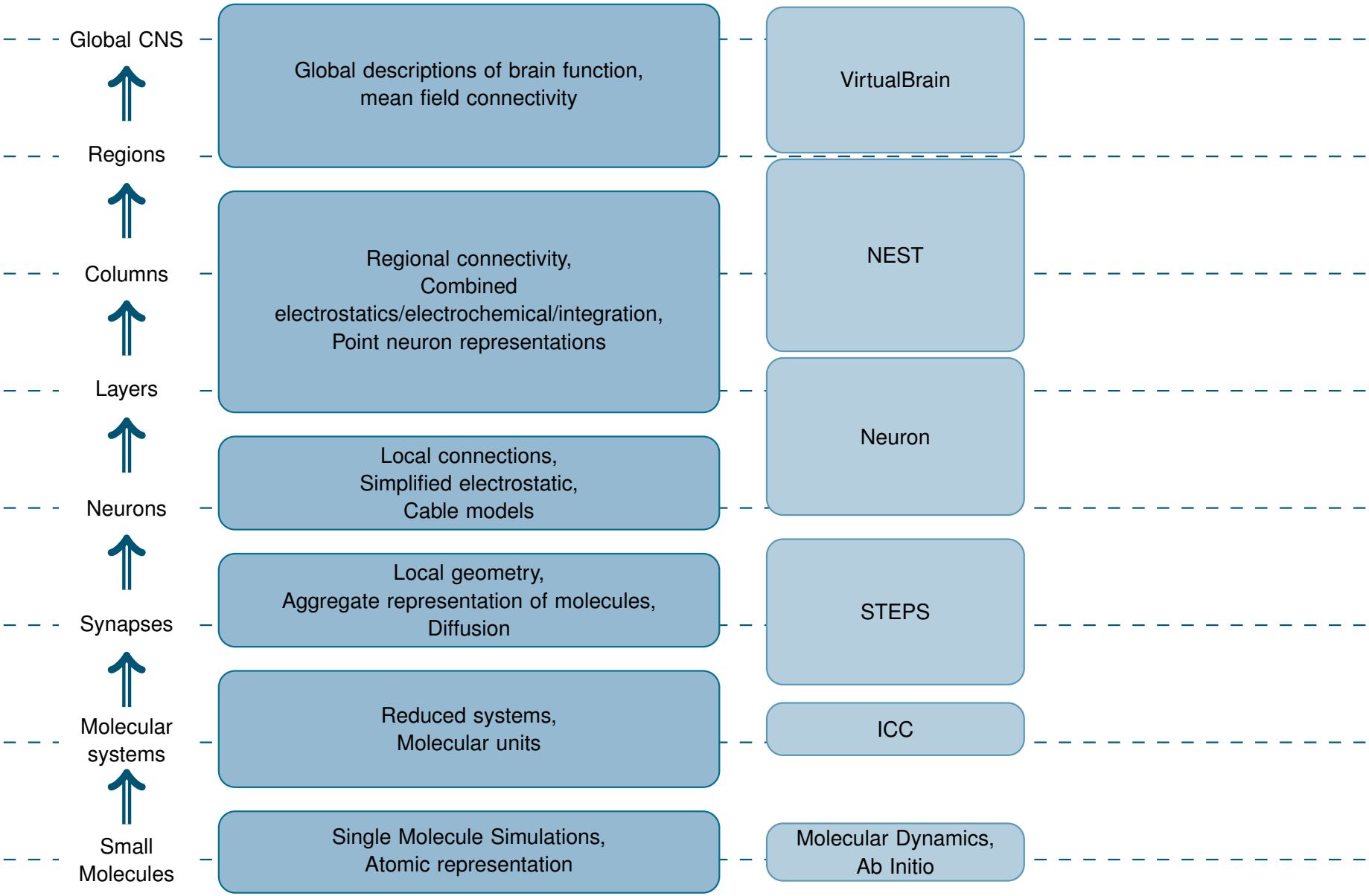

Multiscaling the Nervous System

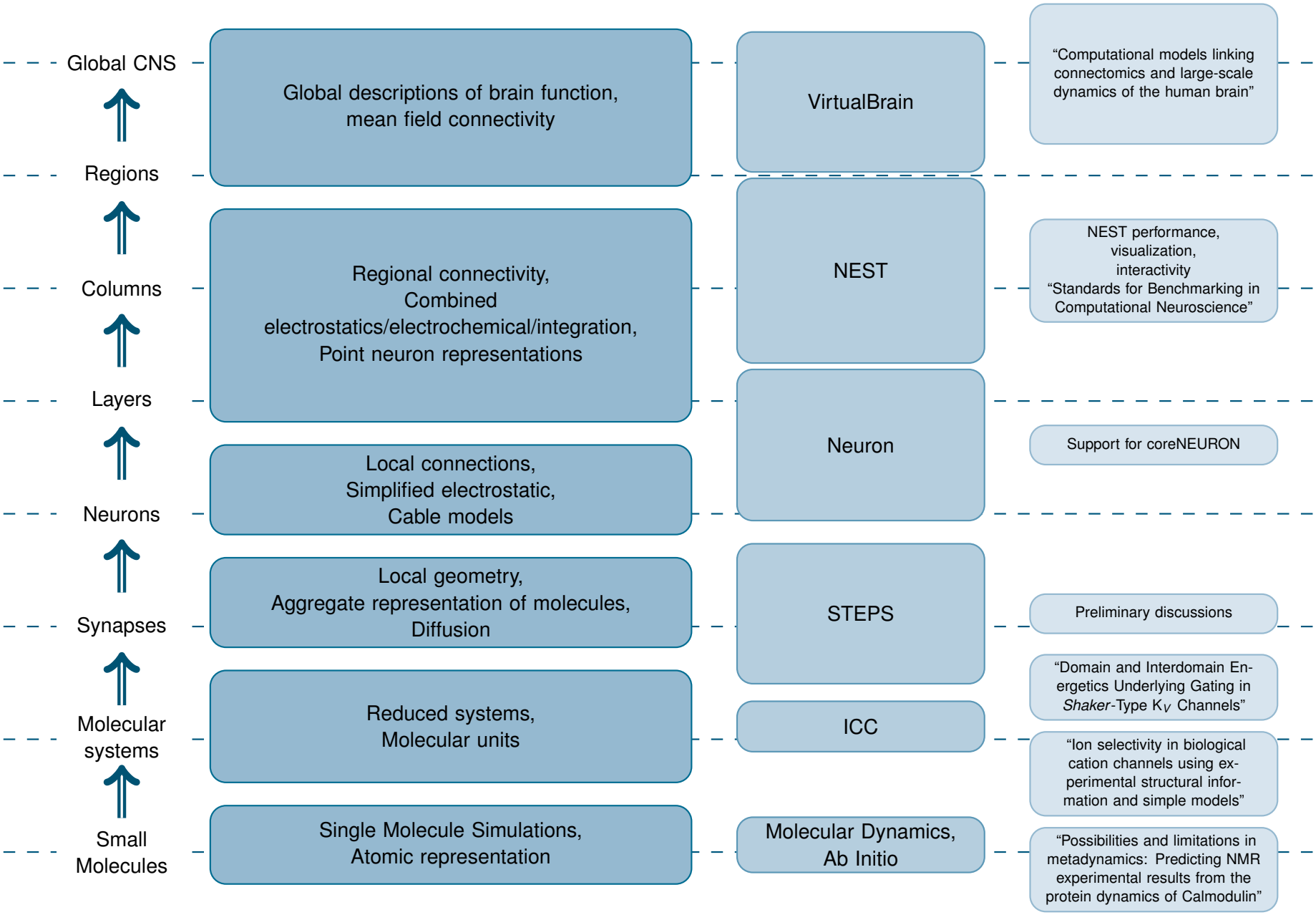

Multiscaling the Nervous System

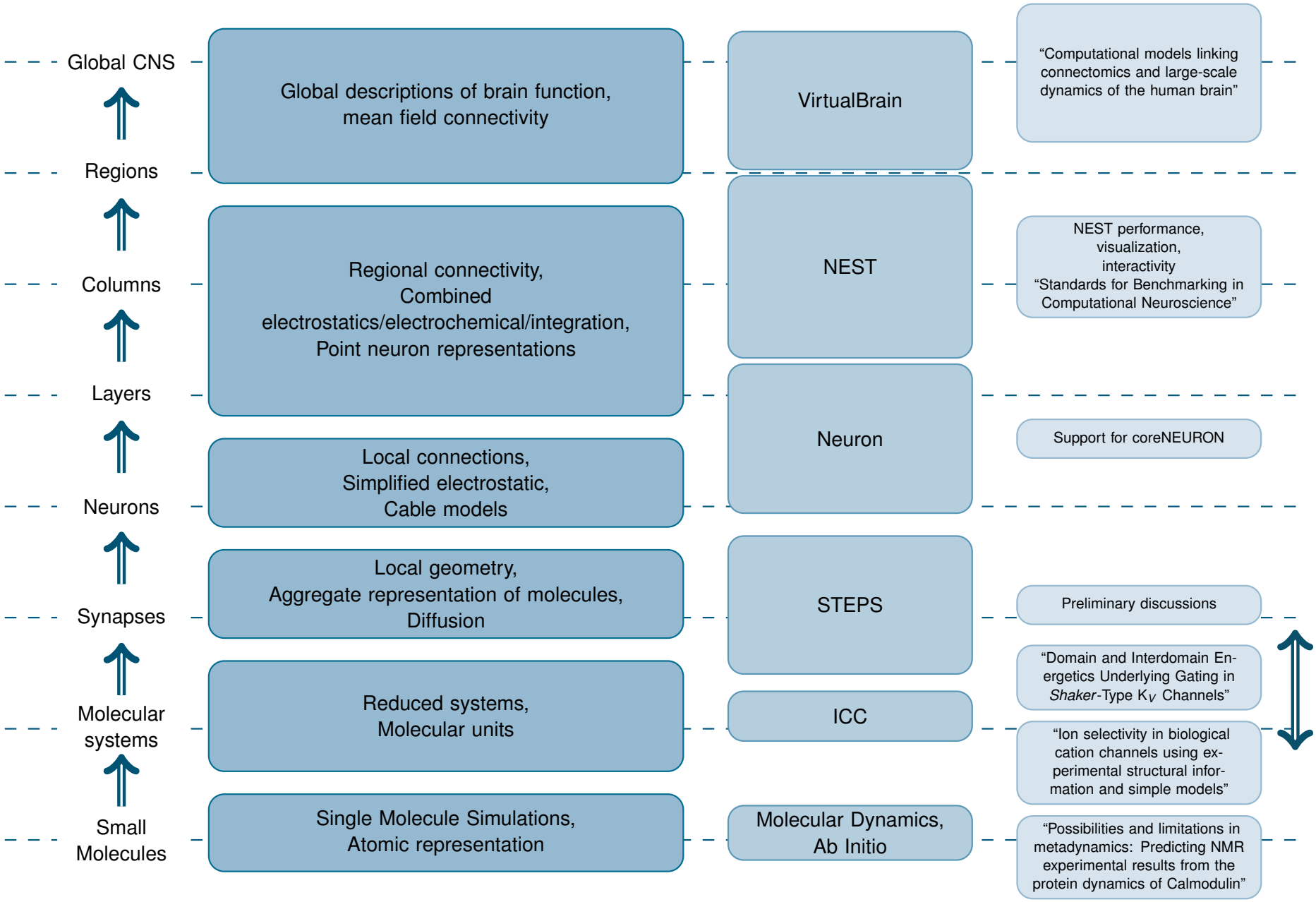

Voltage Gated Currents & Displacements

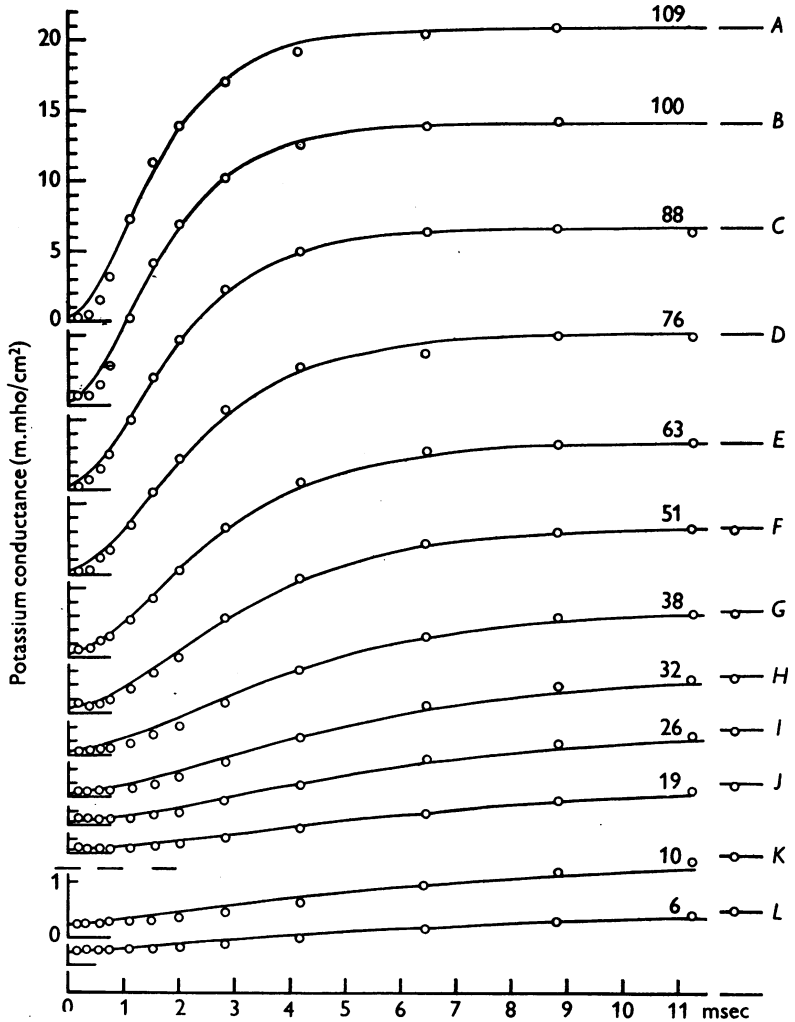

Hodgkin and Huxley (1952, Fig. 3)

$$g_{\mathrm{K}}(t) = g_{\mathrm{K}\infty}\left\{1 - \left[1 - \sqrt[4]{g_{\mathrm{K}0}/g_{\mathrm{K}\infty}}\right]\exp(-t/\tau_n)\right\}^4$$

Voltage Gated Currents & Displacements

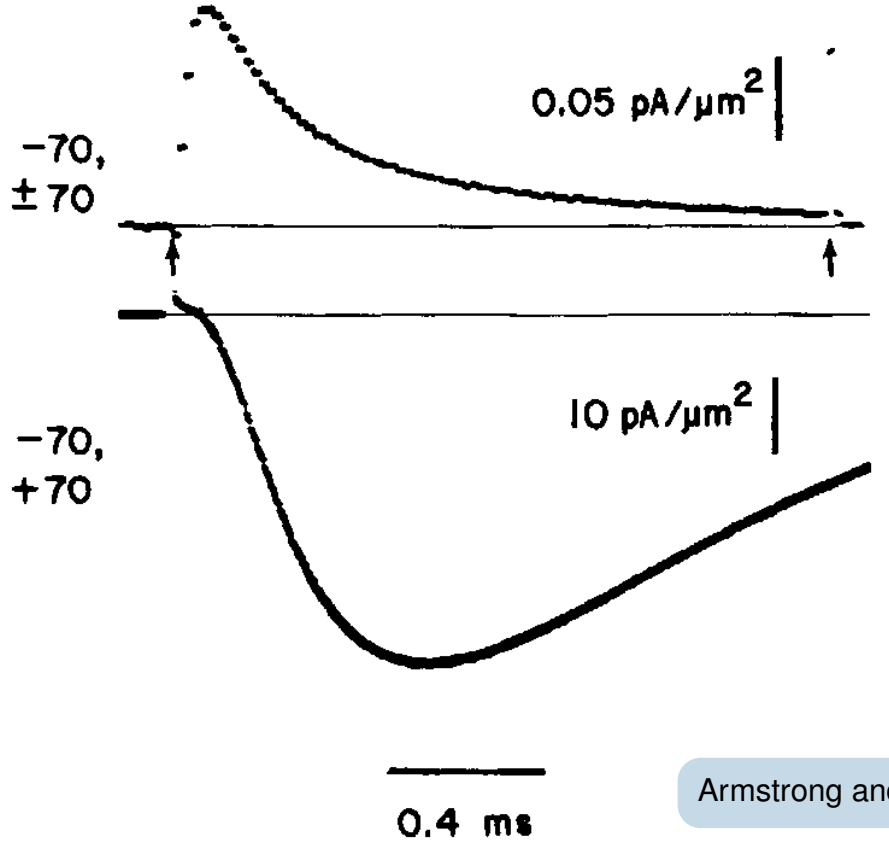

Armstrong and Bezanilla (1973, Fig. 2)

$$g_{\mathrm{K}}(t) = g_{\mathrm{K}\infty}\left\{1 - \left[1 - \sqrt[4]{g_{\mathrm{K}0}/g_{\mathrm{K}\infty}}\right]\exp(-t/\tau_n)\right\}^4$$

Structure

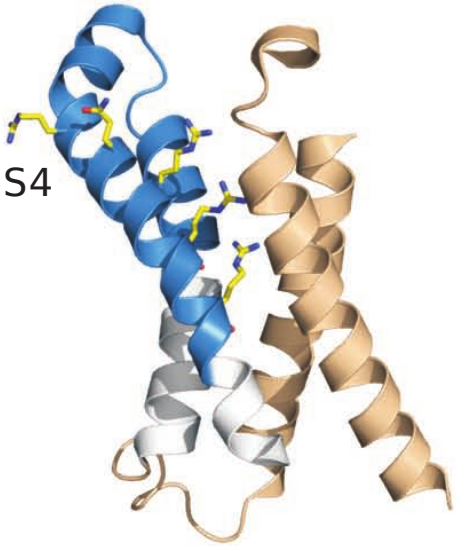

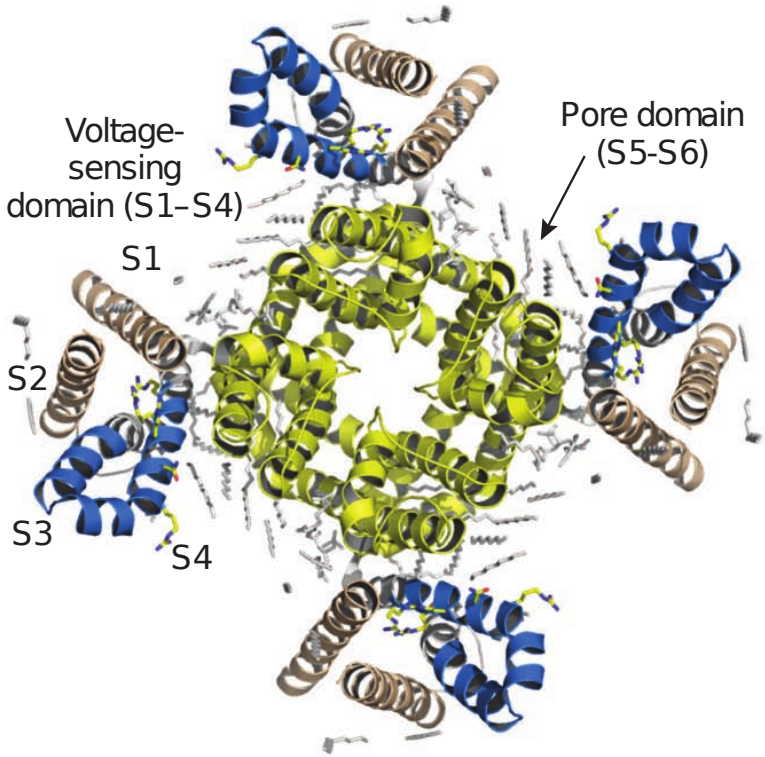

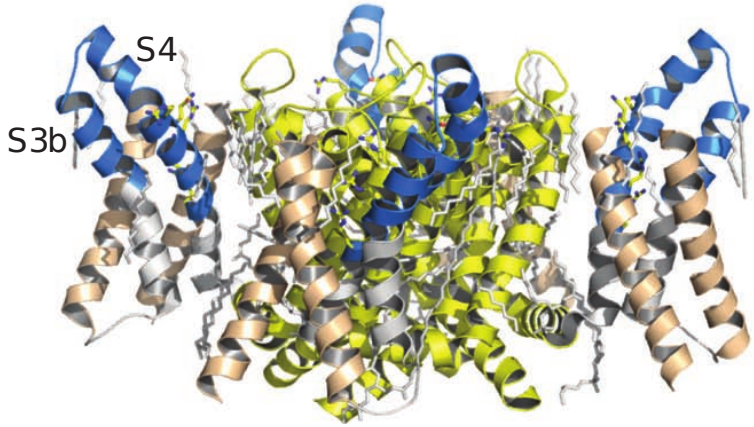

Kalia and Swartz (2013, Fig. 1, 2)

Multiscale gating

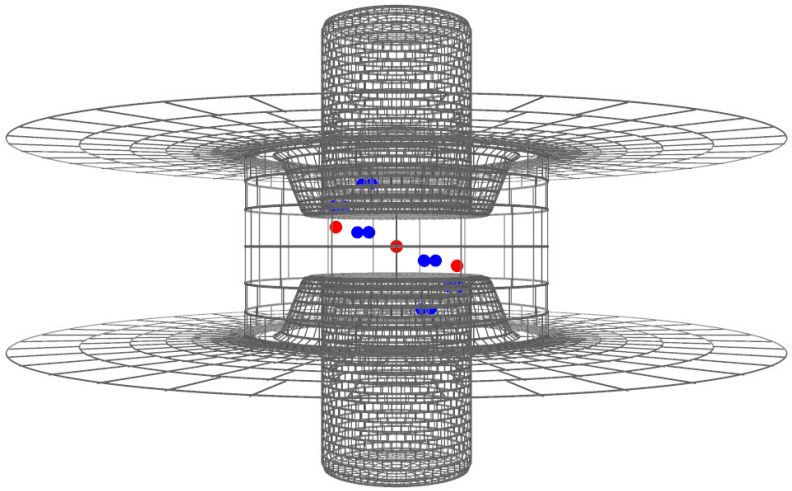

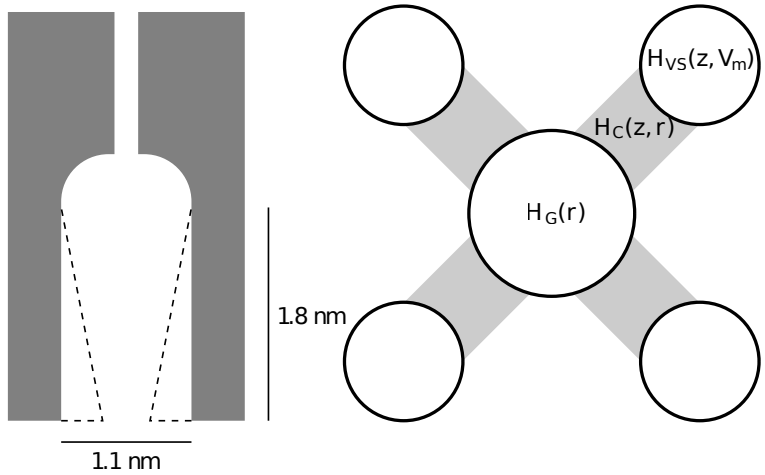

$$B(\mathbf{z}, r, V_\mathrm{m}) = \exp\{-\beta[\mathcal{H}_\mathrm{G}(r) + \sum_{i=1}^{4}(\mathcal{H}_{\mathrm{C},i}(z_i, r) + \mathcal{H}_{\mathrm{B},i}(z_i) + \mathcal{H}_{\mathrm{VS},i}(z_i, V_\mathrm{m}))]\}$$

$$\mathcal{H}_{\mathrm{VS},i}(z_i, V_\mathrm{m}) = -\beta^{-1} \ln \sum_j \exp\left[-\beta \mathcal{H}_{\mathrm{VS},i}(z_i, \phi_j, V_\mathrm{m})\right]$$

Voltage Sensor Model

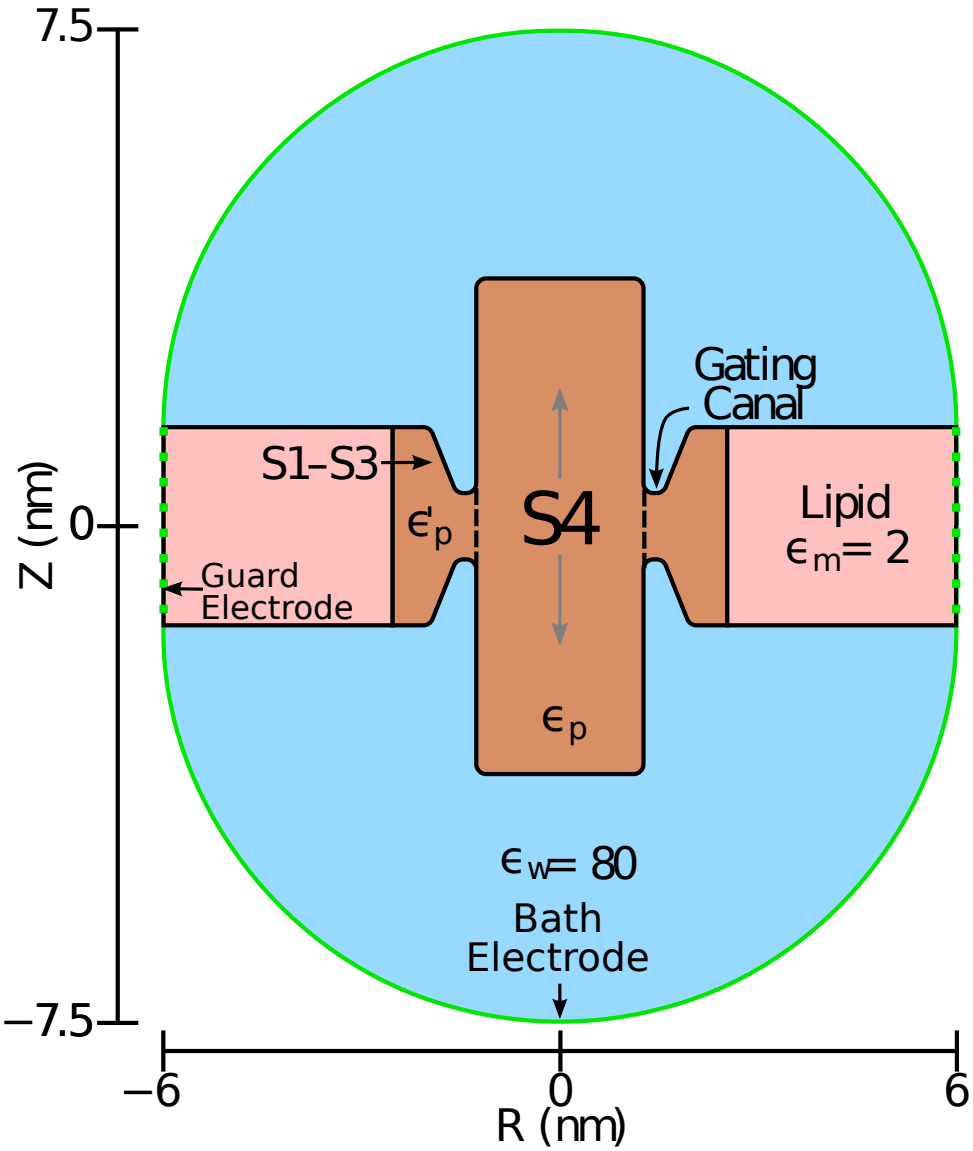

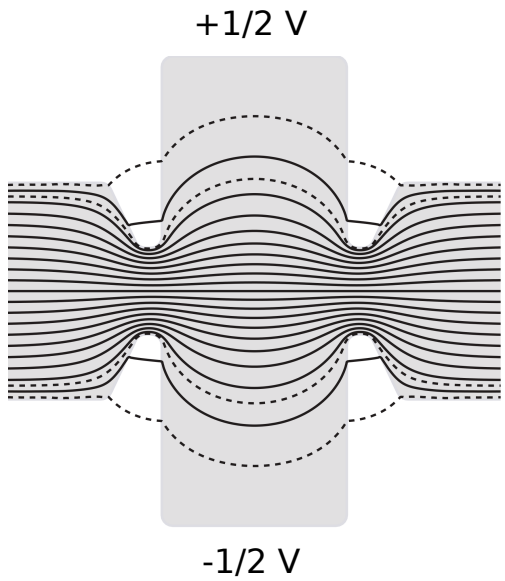

Peyser and Nonner (2012, Fig. 1)

Nonner et al. (2004, Fig. 3B)

Gate Model

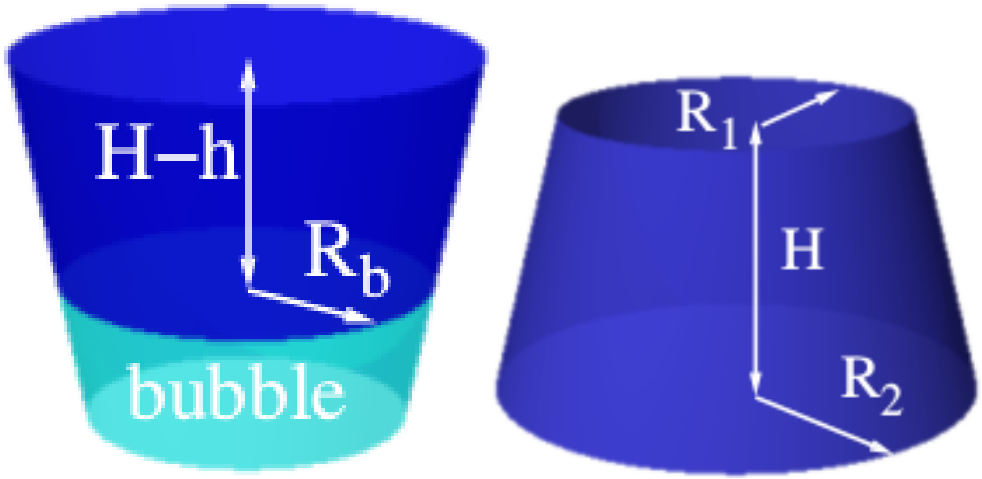

Roth et al. (2008)

$$P_{\text{open}}(R_2) = (1 + \exp(-\beta \Delta\Omega(R_2)))^{-1}$$

$$\Omega_{\text{gate}}^{\text{open}} = -p_l V(H, R_1, R_2) + \sigma_l M(H, R_1, R_2) + \kappa_l C(H, R_1, R_2)$$

$$\begin{aligned}\Omega_{\text{gate}}^{\text{closed}} = &- p_l V(H-h, R_1, R_b) + \sigma_l M(H-h, R_1, R_b) + \kappa_l C(H-h, R_1, R_b) \\ &- p_g V(h, R_b, R_2) + \sigma_g M(h, R_b, R_2) + \kappa_g C(H-h, R_b, R_2) \\ &+ \sigma_{gl}(A(R_b) + A(R_2))\end{aligned}$$

Hamiltonians & Component Inputs

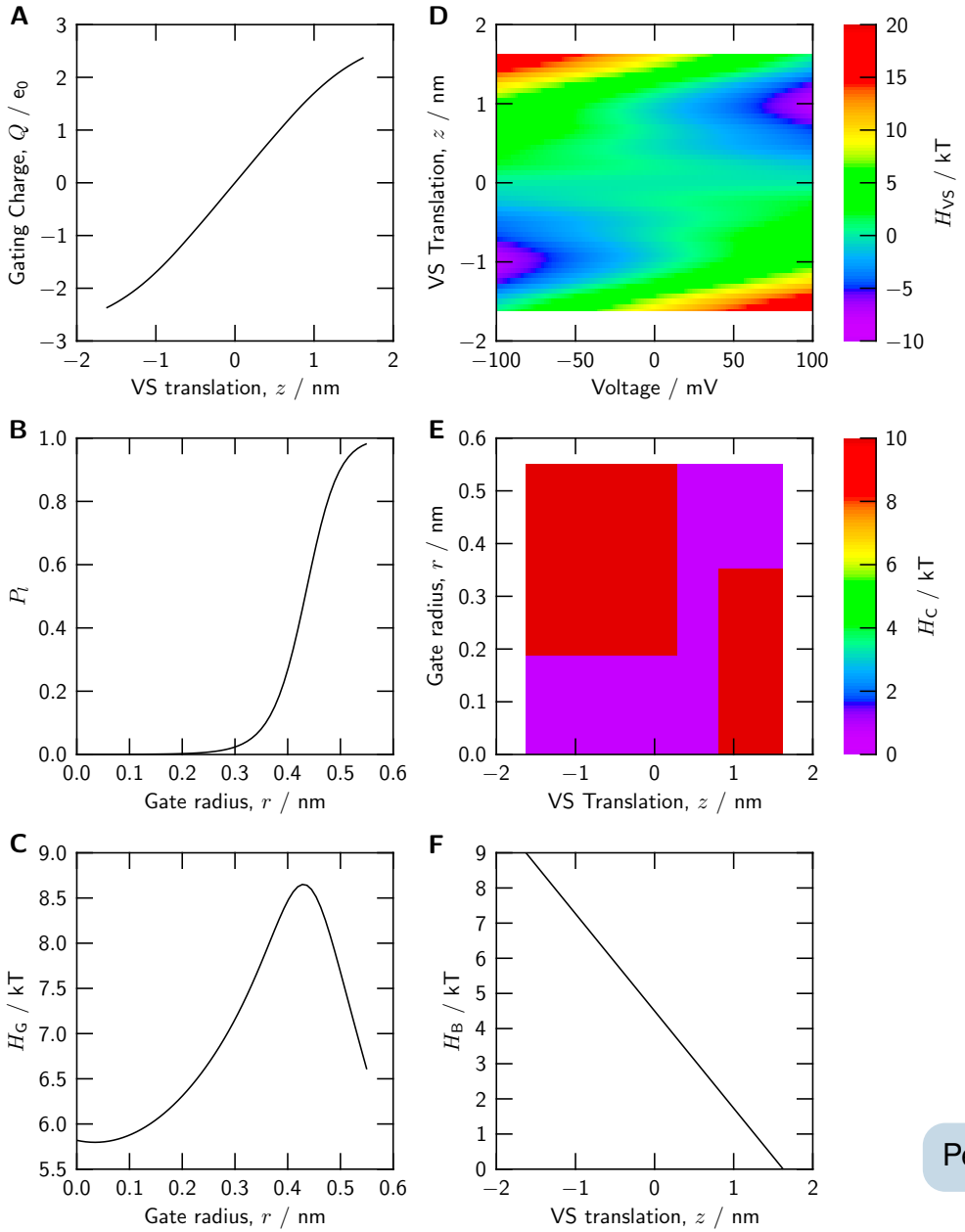

Peyser et al. (2014, Fig. 2)

Full-channel experimental predictions

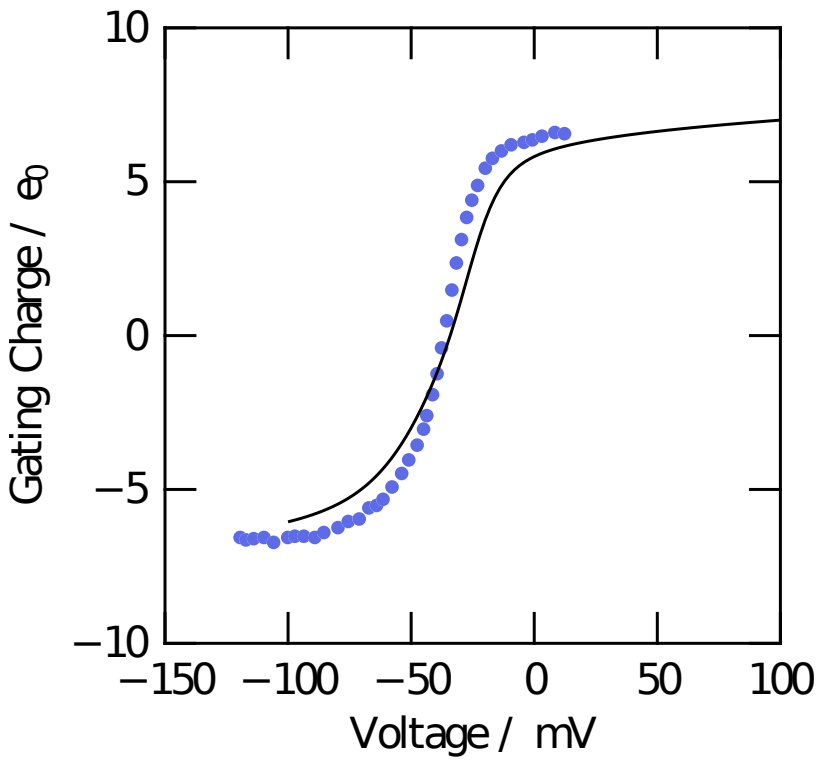

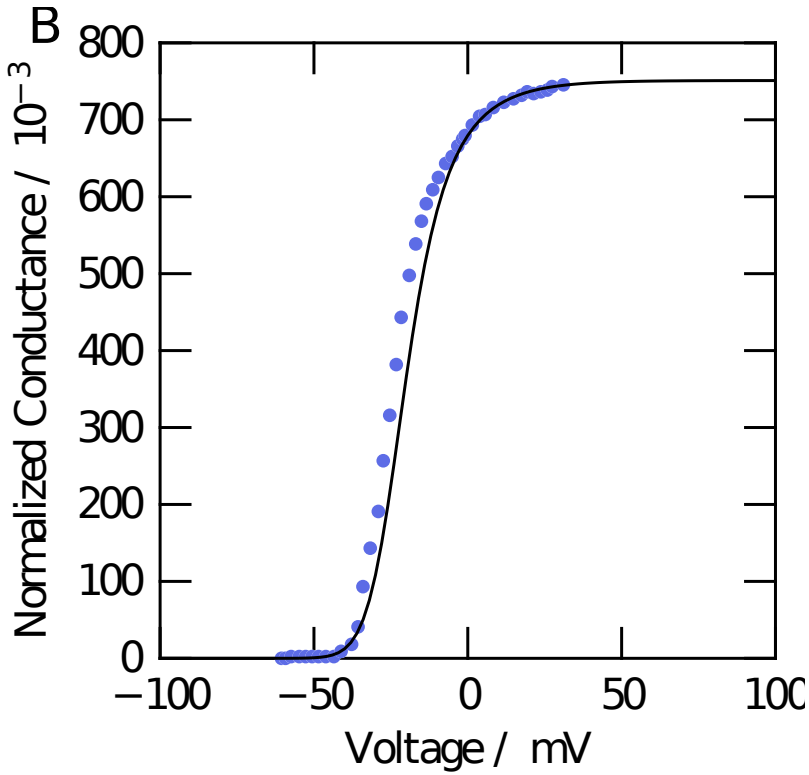

Peyser et al. (2014, Fig. 3, black lines)

Seoh et al. (1996, Fig. 2, blue points)

$$\mathcal{Q}(V_\mathrm{m}) = \sum_{I=1}^{N_r} \sum_{k_1=1}^{N_z} \sum_{k_2=k_1}^{N_z} \sum_{k_3=k_2}^{N_z} \sum_{k_4=k_3}^{N_z} n(k_1, k_2, k_3, k_4) B(z_{k_1}, z_{k_2}, z_{k_3}, z_{k_4}, r_I, V_\mathrm{m})$$

The Critical Gap

Building H&H from subcellular components

JÜLICH FORSCHUNGSZENTRUM

Subcellular simulations: the problem

NEST can handle complex networks

NEURON can represent generic neuronal geometry

Gap ↕ molecular assemblages, organelles, subcellular structures mass diffusion

Atomistic simulations can not be used to build up macro-molecular structures and organelles

The Critical Gap

Building H&H from subcellular components

JÜLICH FORSCHUNGSZENTRUM

Subcellular simulations: some solutions

Dryga et al. (2012)	Realistic simulation of the activation of voltage-gated ion channels. Proc Natl Acad Sci U S A, 109(9):3335–3340, 2012.
Lopreore et al. (2008)	Computational modeling of three-dimensional electrodiffusion in biological systems: Application to the node of Ranvier. Biophys J, 95(6):2624–2635, 2008.
Xylouris et al. (2010)	A three-dimensional mathematical model of active signal processing in axons. Comput Vis Sci, 13(8):409–418, 2010.
Hepburn et al. (2012)	STEPS: efficient simulation of stochastic reaction-diffusion models in realistic morphologies. BMC Syst Biol, 6(1):36, 2012.
Pods et al. (2013)	Electrodiffusion models of neurons and extracellular space using the Poisson-Nernst-Planck equations: numerical simulation of the intra- and extracellular potential for an axon model. Biophys J, 105(1):242–254, 2013.

Acknowledgments

HPC in Neuroscience/SimLab

Boris Orth
Abigail Morrison

University of Miami

Wolfgang Nonner
Karl Magleby
Alice Holohean

Rush University

Bob Eisenberg
Dirk Gillespie

Universität Tübingen

Roland Roth

Funding

Deutsche Forschungsgemeinschaft
Helmholtz Association:
SMBH: Supercomputing and Modelling for Human Brain
JARA: Jülich Aachen Research Alliance
University of Miami
National Institutes of Health
NSF Graduate Research Fellowship
German Research School for Simulation Sciences

Any opinions, findings, conclusions or recommendations expressed in this publication are those of the author and do not necessarily reflect the views of any funders.

References I

C. Armstrong and F. Bezanilla. Currents related to movement of the gating particles of the sodium channels. Nature, 242(5398):459–461, 13 Apr. 1973. doi: 10.1038/242459a0.

A. Dryga, S. Chakrabarty, S. Vicatos, and A. Warshel. Realistic simulation of the activation of voltage-gated ion channels. Proc Natl Acad Sci U S A, 109(9):3335–3340, 2012. doi: 10.1073/pnas.1121094109.

J. J. Finnerty, A. Peyser, and P. Carloni. Ion selectivity in biological cation channels using experimental structural information and simple models. Submitted to: J Phys Chem B, 2015.

I. Hepburn, W. Chen, S. Wils, and E. De Schutter. STEPS: efficient simulation of stochastic reaction-diffusion models in realistic morphologies. BMC Syst Biol, 6(1):36, 2012. ISSN 1752-0509. doi: 10.1186/1752-0509-6-36.

References II

A. Hodgkin and A. Huxley. A quantitative description of membrane current and its application to conduction and excitation in nerve. J Physiol, 117(4):500–544, 1952. ISSN 00223751. URL http://www.ncbi.nlm.nih.gov/pmc/articles/PMC1392413.

J. Kalia and K. J. Swartz. The design principle of paddle motifs in voltage sensors. Nat Struct Mol Biol, 20(5):534–535, May 2013. ISSN 1545-9993. doi: 10.1038/nsmb.2578.

C. L. Lopreore, T. M. Bartol, J. S. Coggan, D. X. Keller, G. E. Sosinsky, M. H. Ellisman, and T. J. Sejnowski. Computational modeling of three-dimensional electrodiffusion in biological systems: Application to the node of Ranvier. Biophys J, 95(6):2624–2635, 2008. ISSN 0006-3495. doi: 10.1529/biophysj.108.132167.

W. Nonner, A. Peyser, D. Gillespie, and B. Eisenberg. Relating microscopic charge movement to macroscopic currents: The Ramo-Shockley theorem applied to ion channels. Biophys J, 87(6): 3716–3722, 2004. ISSN 0006-3495. doi: 10.1529/biophysj.104.047548.

References III

A. Peyser. Possibilities and limitations in metadynamics: Predicting NMR experimental results from the protein dynamics of Calmodulin. In Production, 2015.

A. Peyser and W. Nonner. Voltage sensing in ion channels: Mesoscale simulations of biological devices. Phys Rev E Stat Nonlin Soft Matter Phys, 86:011910, July 2012. doi: 10.1103/PhysRevE.86.011910.

A. Peyser, D. Gillespie, R. Roth, and W. Nonner. Domain and inter-domain energetics underlying gating in *Shaker*-type K_v channels. Biophys J, 107(8):1841–1852, 2014. doi: 10.1016/j.bpj.2014.08.015.

A. Peyser, Y. Zaytsev, A. Morrison, and M. Diesmann. Standards for benchmarking in computational neuroscience. In Production, 2015.

J. Pods, J. Schönke, and P. Bastian. Electrodiffusion models of neurons and extracellular space using the Poisson-Nernst-Planck equations: Numerical simulation of the intra- and extracellular potential for an axon model. Biophys J, 105(1):242–254, 2013. ISSN 0006-3495. doi: 10.1016/j.bpj.2013.05.041.

References IV

R. Roth, D. Gillespie, W. Nonner, and R. E. Eisenberg. Bubbles, gating, and anesthetics in ion channels. Biophys J, 94(11):4282–4298, 2008. ISSN 0006-3495. doi: 10.1529/biophysj.107.120493.

S.-A. Seoh, D. Sigg, D. M. Papazian, and F. Bezanilla. Voltage-sensing residues in the S2 and S4 segments of the *Shaker* K^+ channel. Neuron, 16(6):1159–1167, 1 June 1996. ISSN 0896-6273. doi: 10.1016/S0896-6273(00)80142-7.

K. Xylouris, G. Queisser, and G. Wittum. A three-dimensional mathematical model of active signal processing in axons. Comput Vis Sci, 13(8):409–418, 2010. ISSN 1432-9360. doi: 10.1007/s00791-011-0155-7.

JÜLICH
FORSCHUNGSZENTRUM

Multiscaling the Human Brain

July 21, 2014 | Alexander Peyser | Simulation Lab Neuroscience, Forschungszentrum Jülich

What do I mean?

JÜLICH FORSCHUNGSZENTRUM

A multiscale model

is composed of hierarchical levels of models, where “upper levels” invoke constraints and closures to combine “lower levels” into computable systems with high fidelity.

The constraints and closures are physical laws and model constraints.

The goal is systems that can be computed within reasonable time and with as good or better fidelity than a primitive model for measures of interest.

Why multiscale?

- The space to be searched goes as a power of the number of dimensions to be searched: for example $\mathcal{O}(c^n)$ for isotropic flat spaces with a similar size.
- For many spaces, the low energy region becomes a smaller fraction of the total space by the same function

Approximate scales

Simple protein	10^3
Ion channel	10^4
Ribosome	10^5 + associated proteins
RBC	10^{12}
Neuron	10^{17}
Column	$\approx 10^{20}$
Rodent brain	10^{22}
Human brain	10^{25}

Jarzynski Equation

JÜLICH FORSCHUNGSZENTRUM

The free energy between state A and B, which may or may not be at equilibrium:

$$\exp(-\Delta F_{\mathcal{T}}/kT) = \overline{\exp(-W_{\mathcal{T}}/kT)}$$

This is true for systems that sample their phase space according to the Boltzmann factor:

$$Pr(\mathcal{T}) = \frac{\exp(-\Delta E_{\mathcal{T}}/kT)}{\sum_i \exp(-\Delta E_i/kT)}$$

If we have a system with many trajectories between states and a large fluctuation in work along them ($\sigma \gg kT$), ΔF will be dominated by statistically unlikely low energy pathways.

Calmodulin: An Intrinsically Disordered Protein

JÜLICH FORSCHUNGSZENTRUM

Mass	16706 Daltons
Amino Acids	148
Atoms	1100
Structure	Two globular 'heads' connected by a flexible linker (14 aa)
States	binds Ca^{2+} and ubiquitously peptides in a 'compact' state

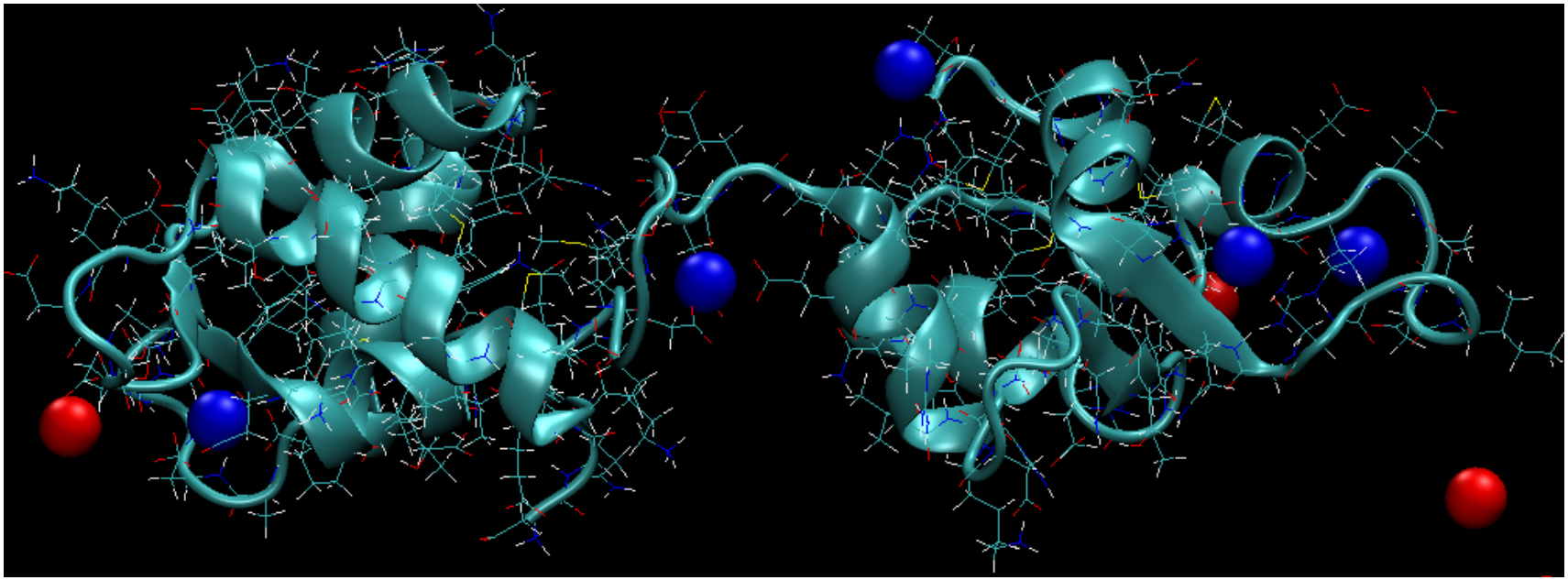

A Metadynamics reduction of molecular dynamics

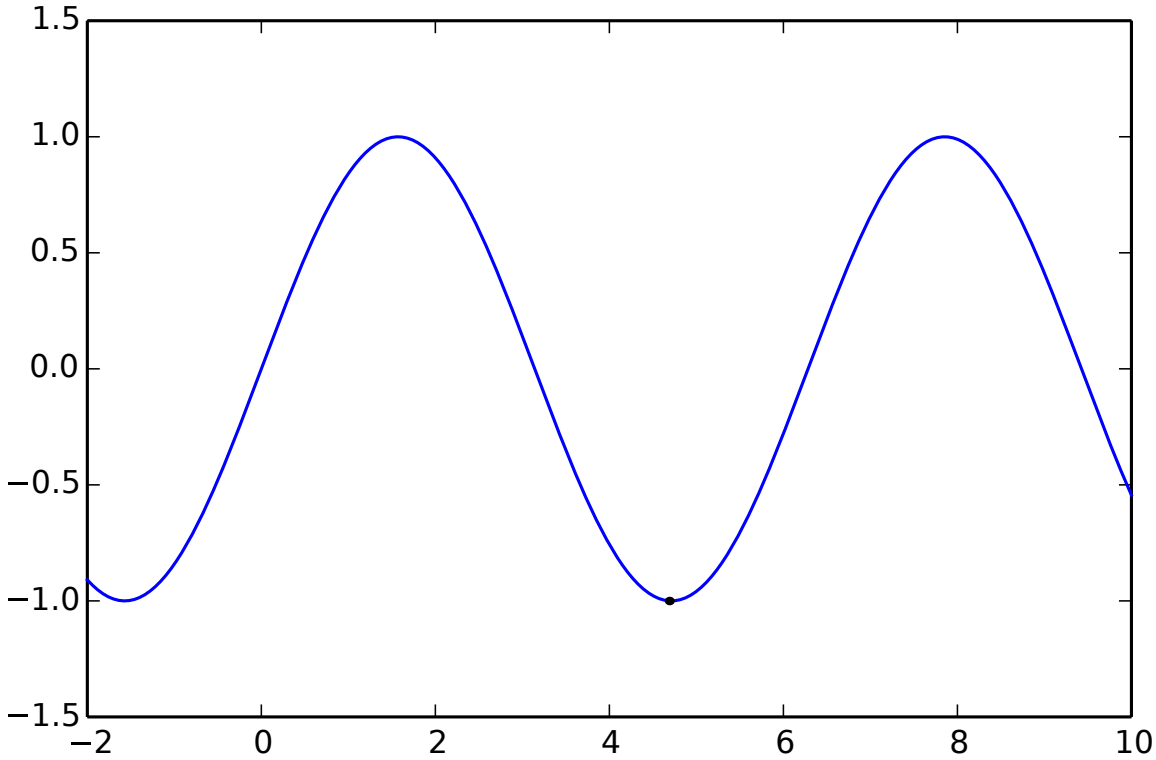

Underlying energy landscape

Metadynamics force field

· Simulation state

A Metadynamics reduction of molecular dynamics

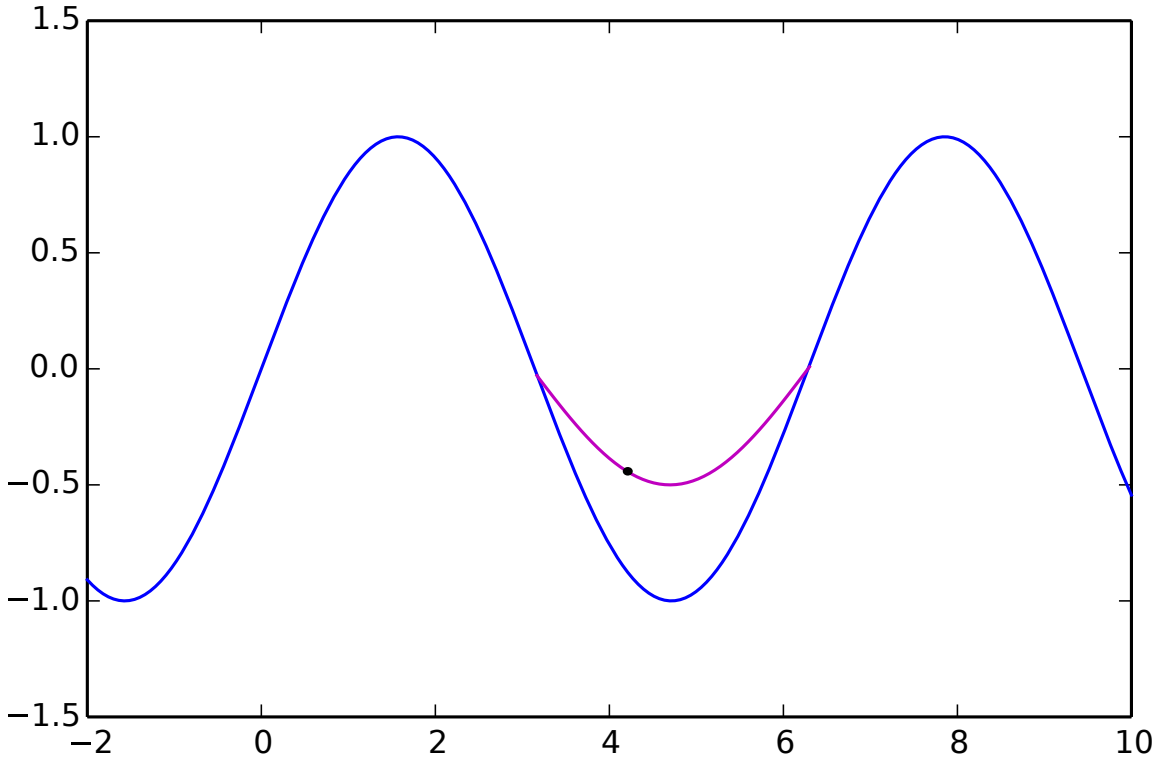

Underlying energy landscape

Metadynamics force field

· Simulation state

A Metadynamics reduction of molecular dynamics

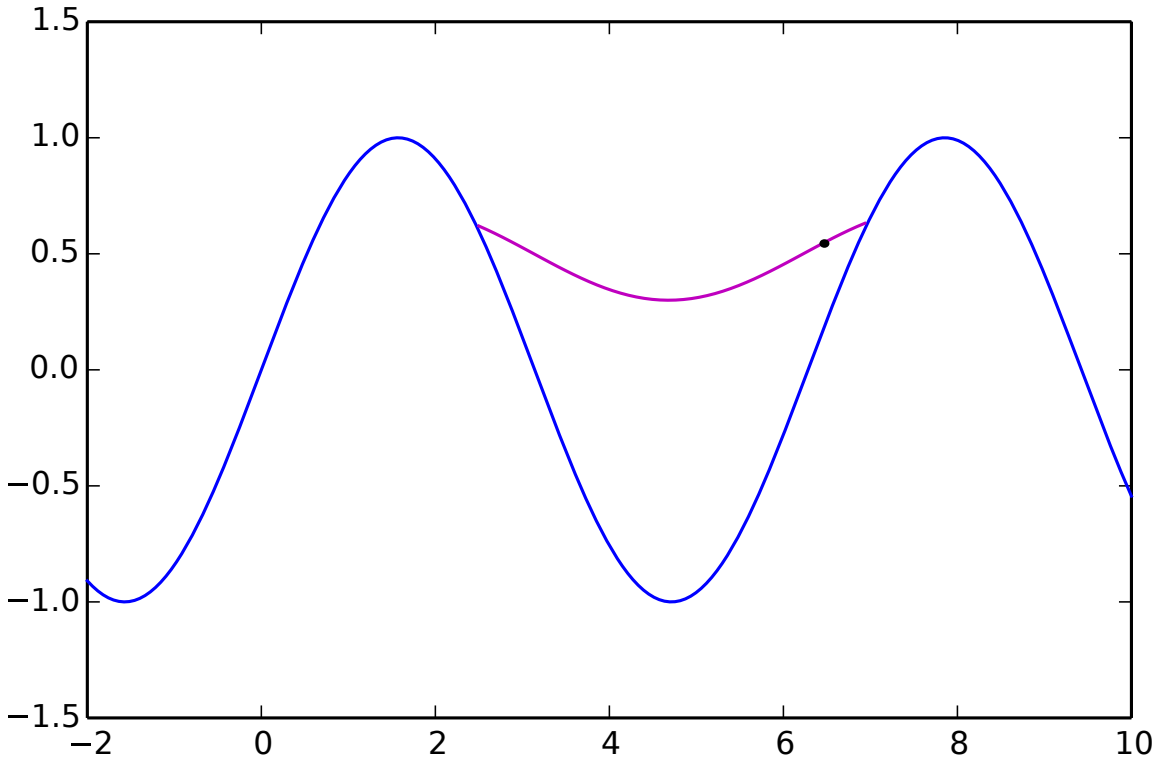

Underlying energy landscape

Metadynamics force field

· Simulation state

A Metadynamics reduction of molecular dynamics

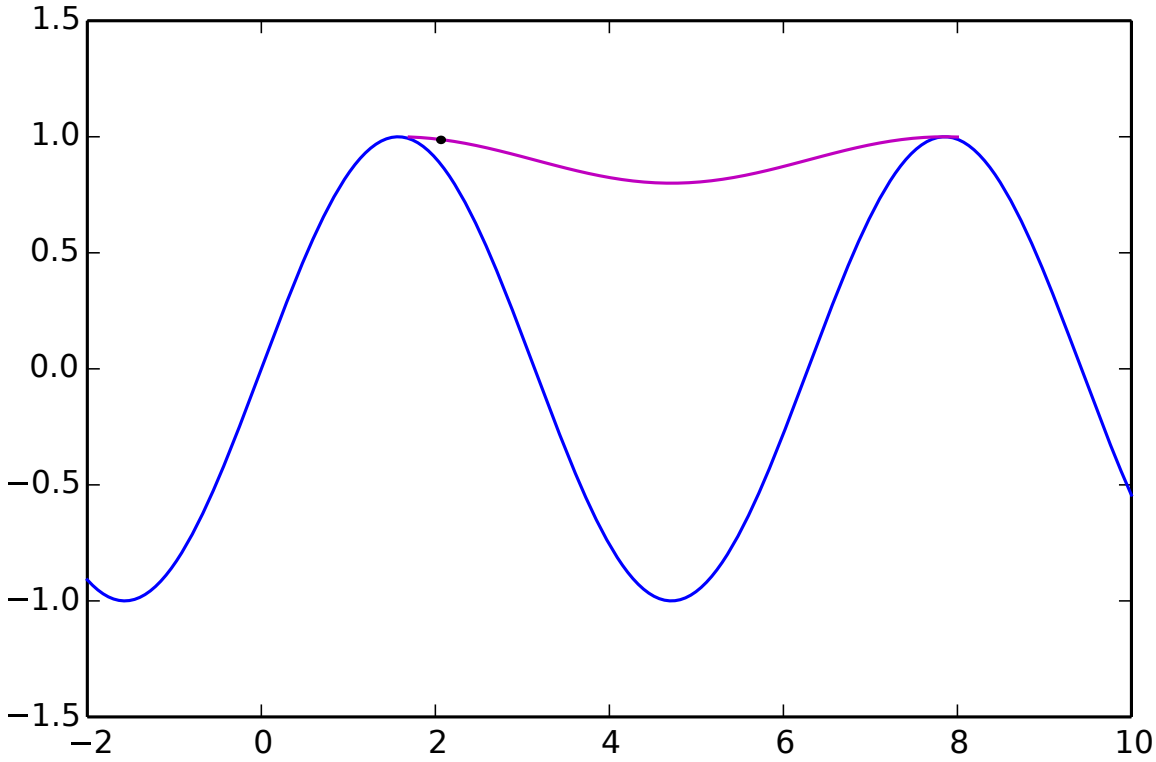

Underlying energy landscape

Metadynamics force field

· Simulation state

A Metadynamics reduction of molecular dynamics

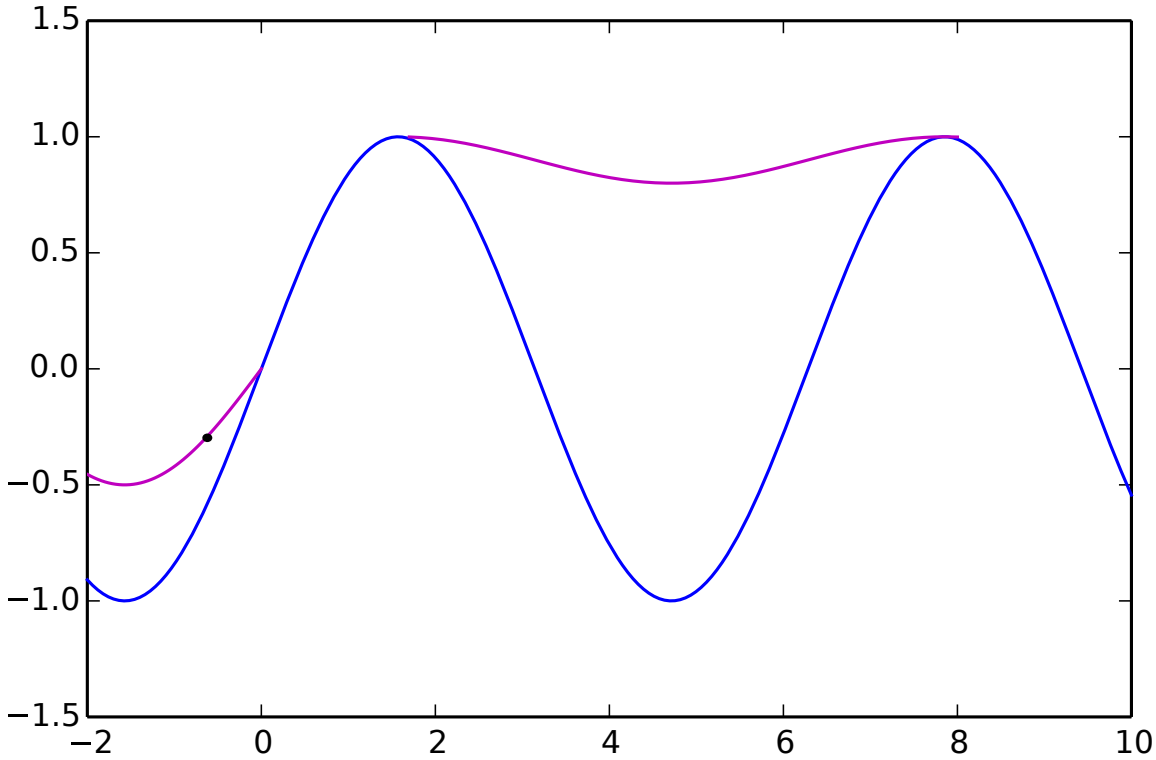

Underlying energy landscape

Metadynamics force field

· Simulation state

Implicit Reduction: The Problem

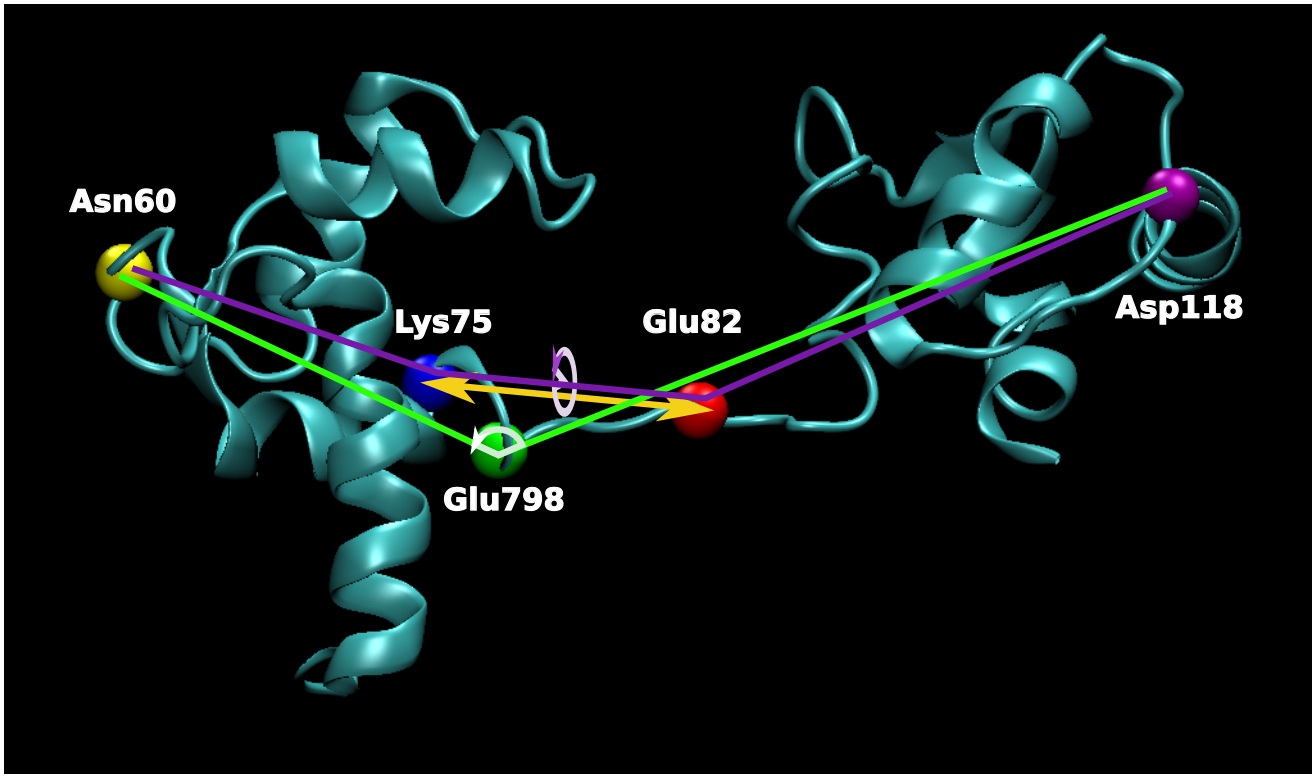

Dimensions

Plane Angle	Asn60–Glu79–Asp118
Dihedral angle	Asn60–Lys74–Glu82–Asp118
Distance	Lys75–Glu82

JÜLICH FORSCHUNGSZENTRUM

NMR

$$C(t) = 1/5\langle P_2(\hat{\mu}_{\mathrm{LF}}(0) \cdot \hat{\mu}_{\mathrm{LF}}(t))\rangle$$

$$J(\omega) = 2\int_0^\infty (\cos\omega t)\; C(t)\; dt$$

PCS

$$\delta^{\mathrm{PCS}} = \frac{1}{12\pi r^3}\left[\Delta\chi_{\mathrm{ax}}(3\cos^2\theta - 1) + \frac{3}{2}\Delta\chi_{\mathrm{rh}}\sin^2\theta\cos 2\varphi\right]$$

RDC

$$\Delta\nu^{\mathrm{RDC}} = -\frac{S_{\mathrm{LS}}}{4\pi}\frac{B_0^2}{15k_BT}\frac{\gamma_{\mathrm{A}}\gamma_{\mathrm{B}}\hbar}{2\pi r_{\mathrm{AB}}^3}$$
$$\left[\Delta\chi_{\mathrm{ax}}(3\cos^2\alpha - 1) + \frac{3}{2}\Delta\chi_{\mathrm{rh}}\sin^2\alpha\cos 2\beta\right]$$

Examples from energy minima

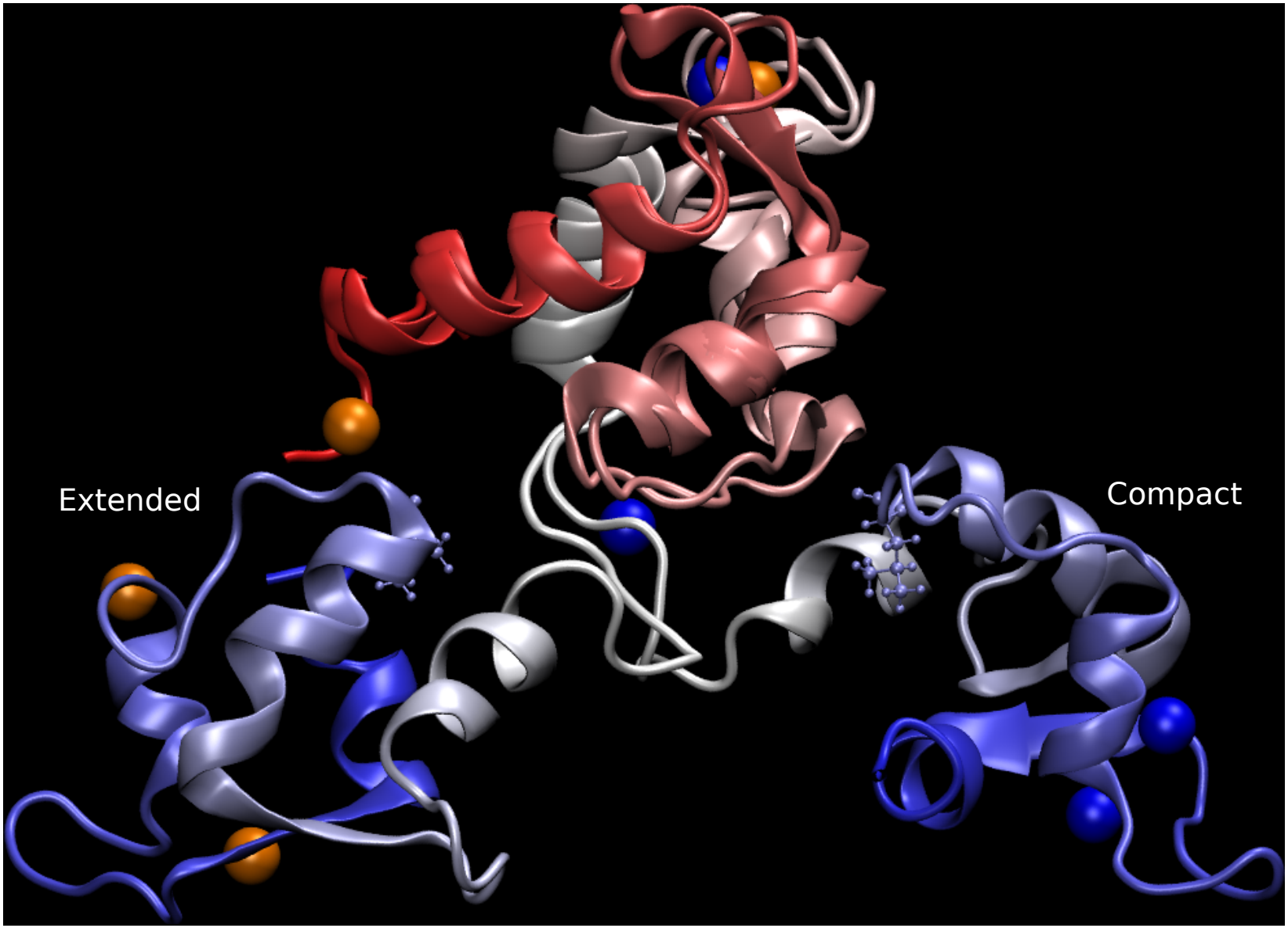

Energy landscapes for axes

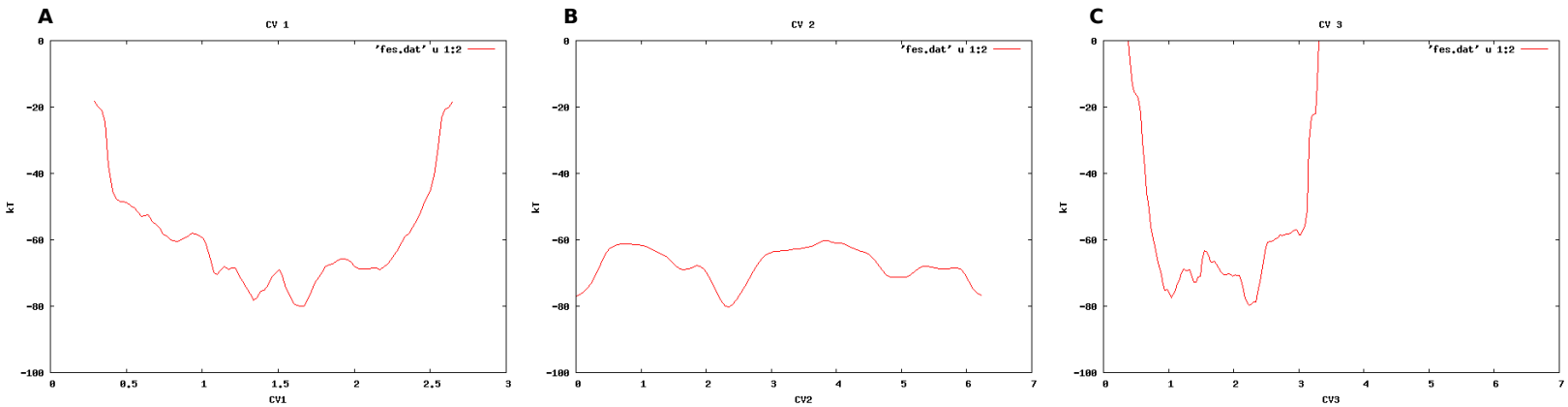

Energy landscapes for axes

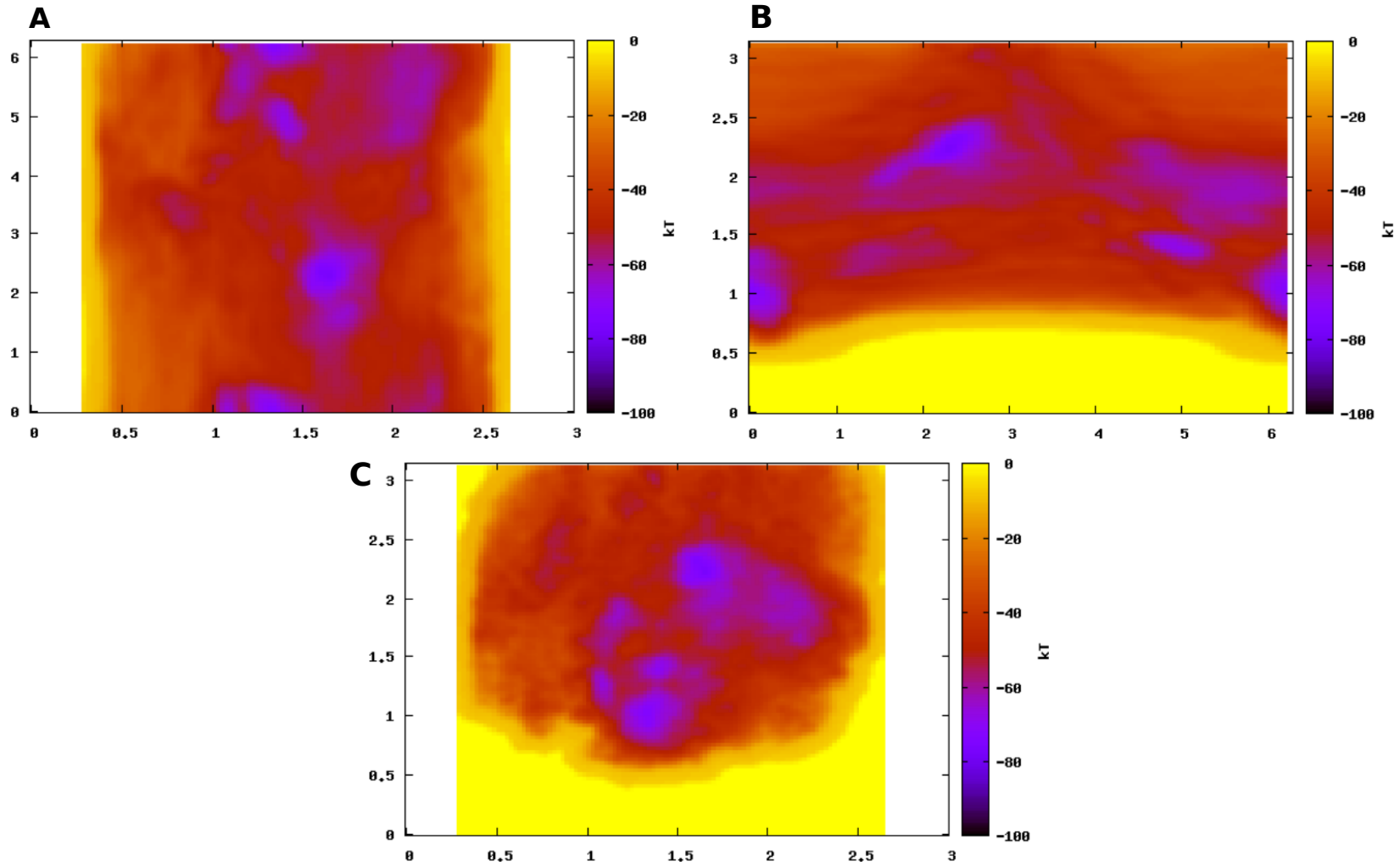

Energy landscapes for axes

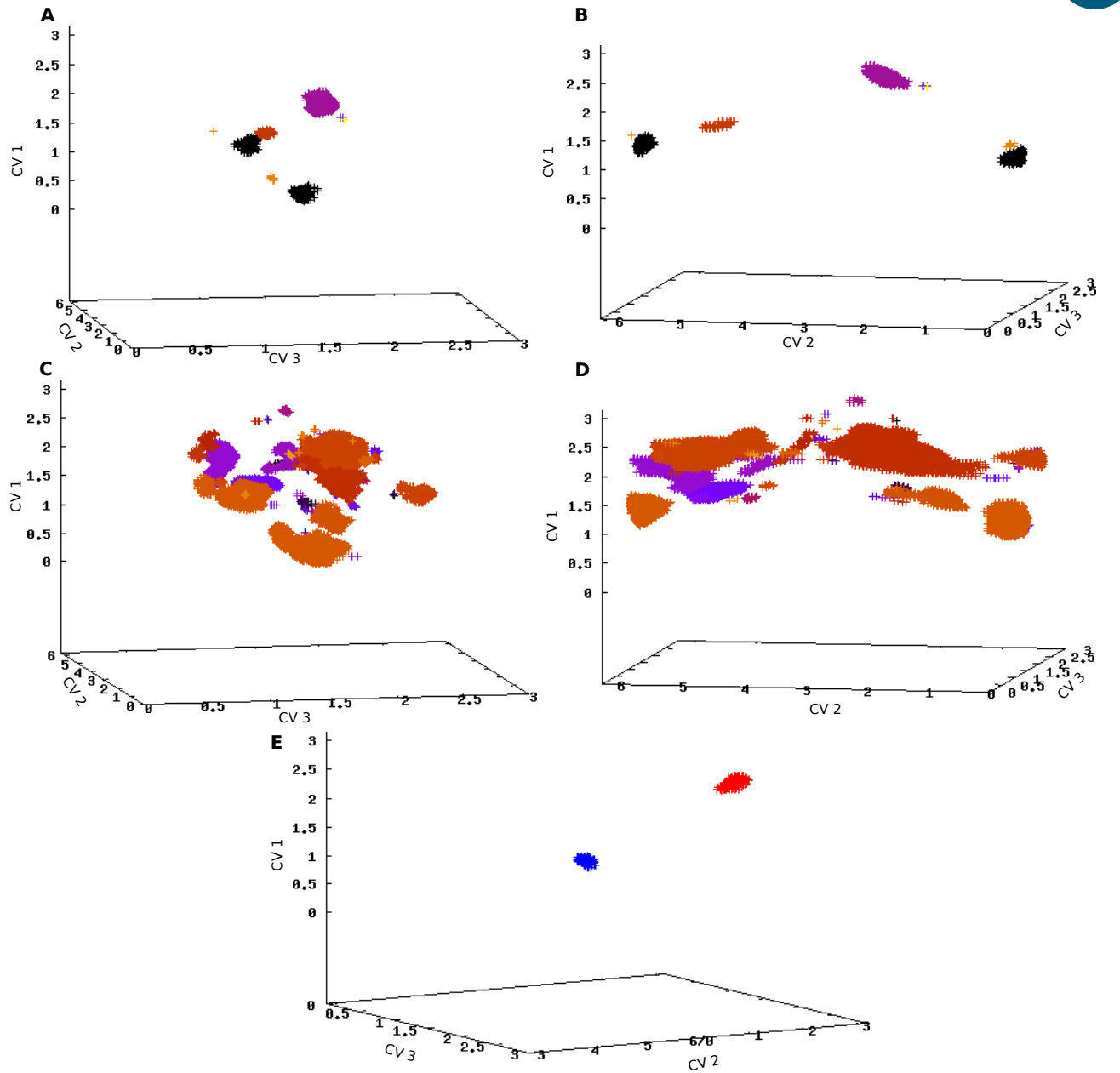

compact
extended

PCS Results

Tb^{3+}

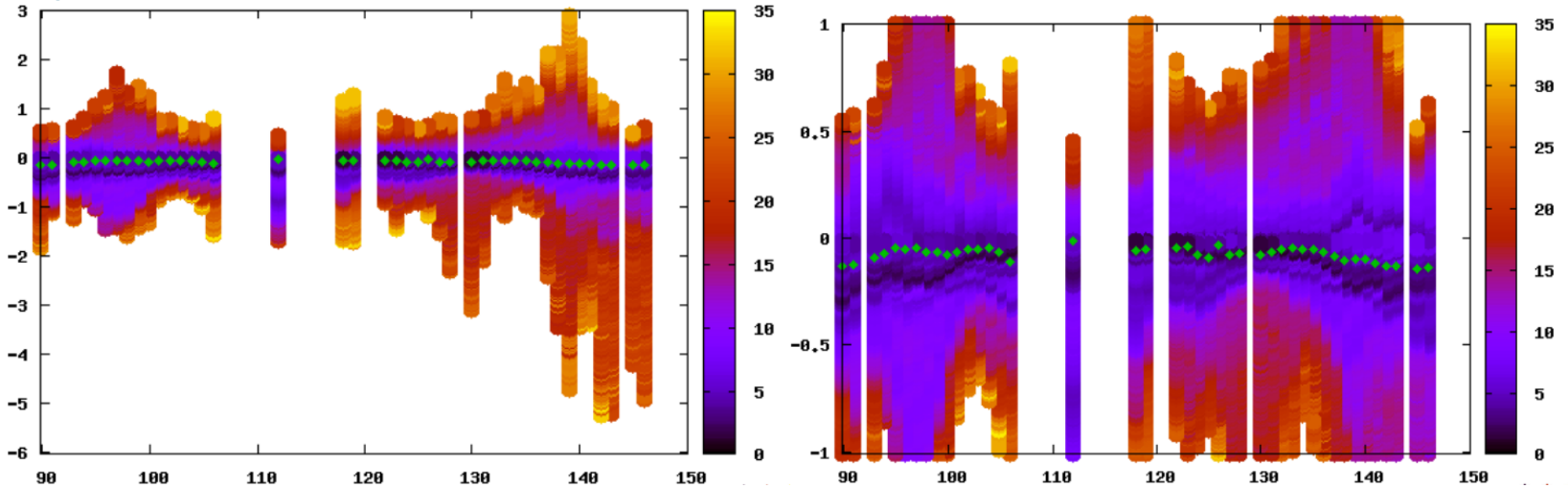

Minima PCS

JÜLICH FORSCHUNGSZENTRUM

Extended

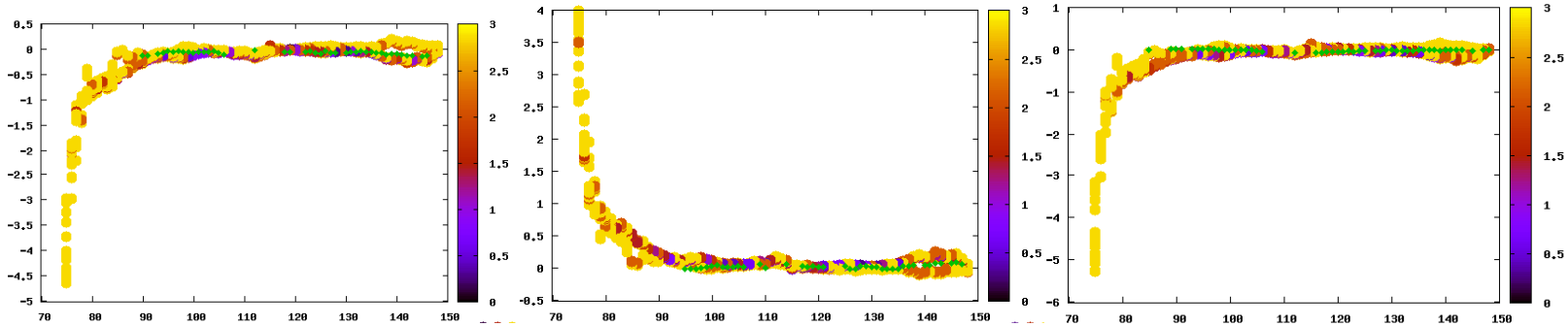

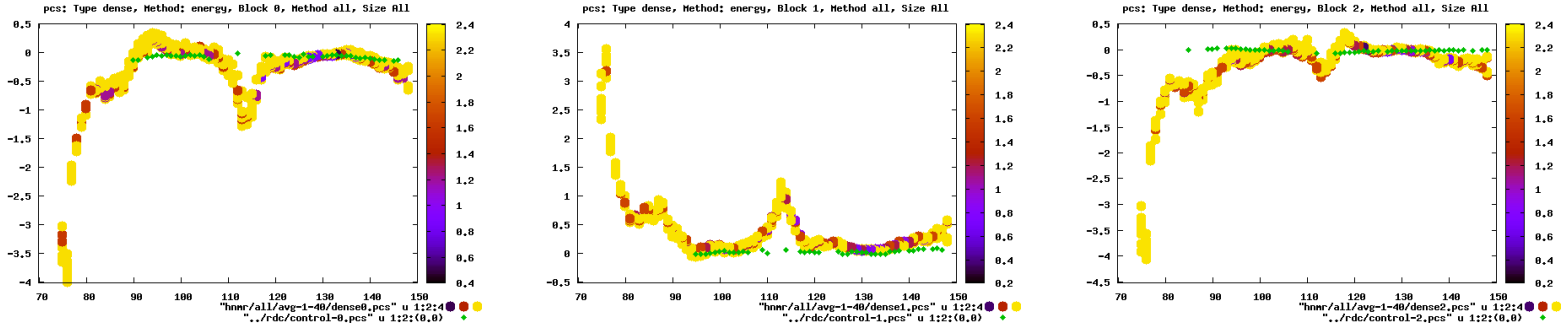

Compact

Surrounding space

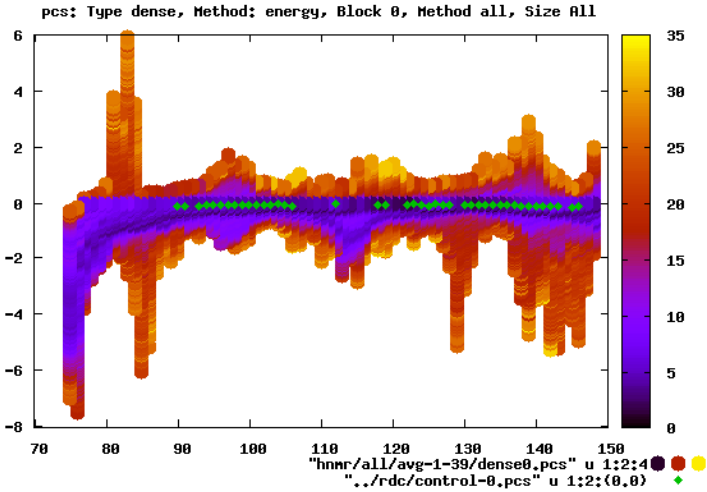

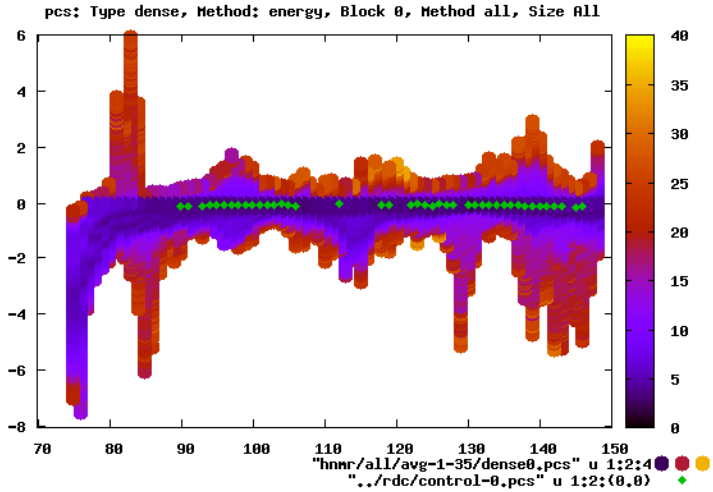

RDC Results

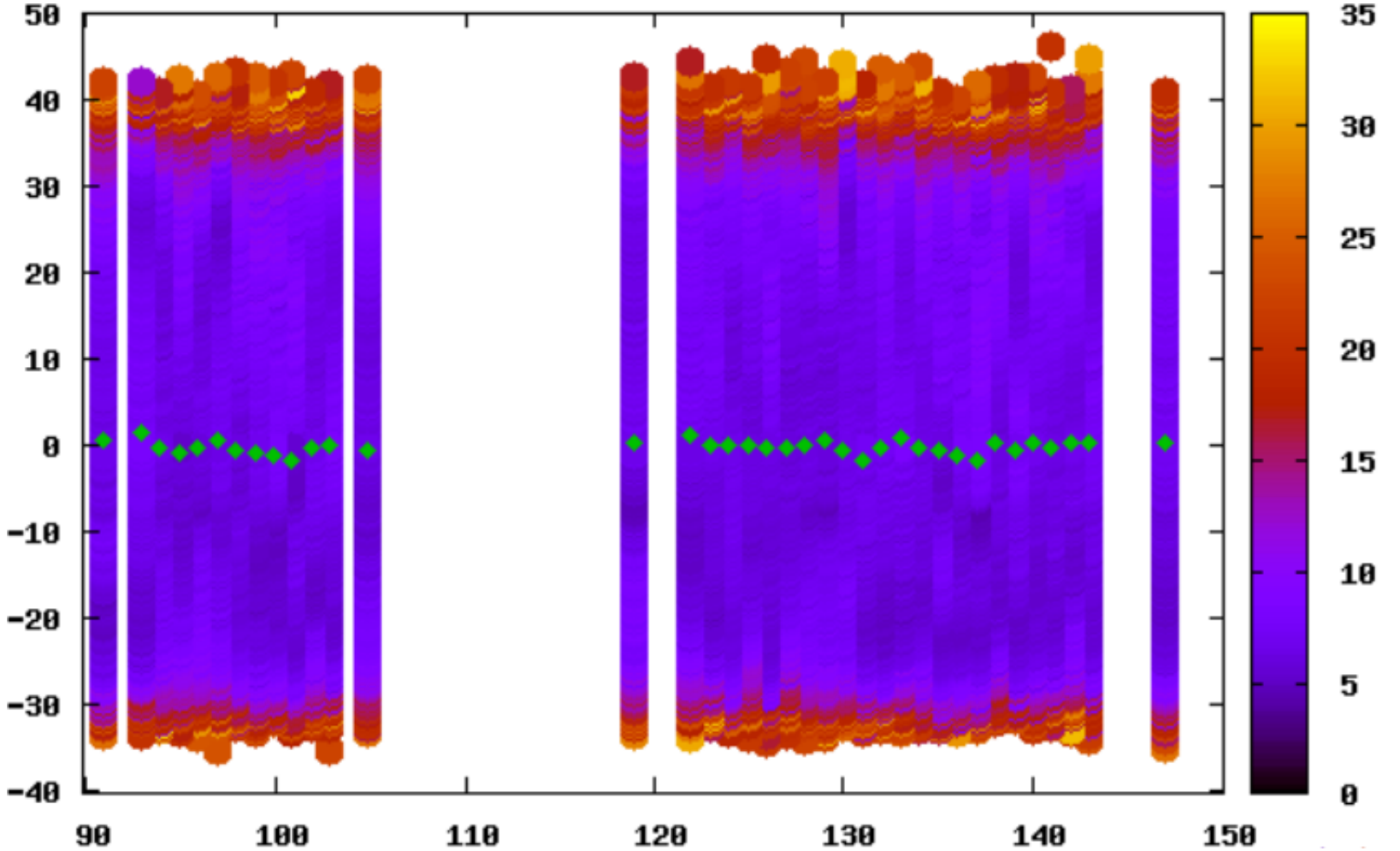
50
40
30
20
10
0
-10
-20
-30
-40
90
100
110
120
130
140
150
35
30
25
20
15
10
5
0

Implications

For this regime

- Flat models of non-homogeneous, non-isotropic and distributed systems may give us good values for specific measurables...

  But...

- Computationally expensive
- Weak “explanatory power”
- May have significant artifacts

Coarse Graining:
Ca^{2+} vs K^{+} vs Na^{+} selectivity

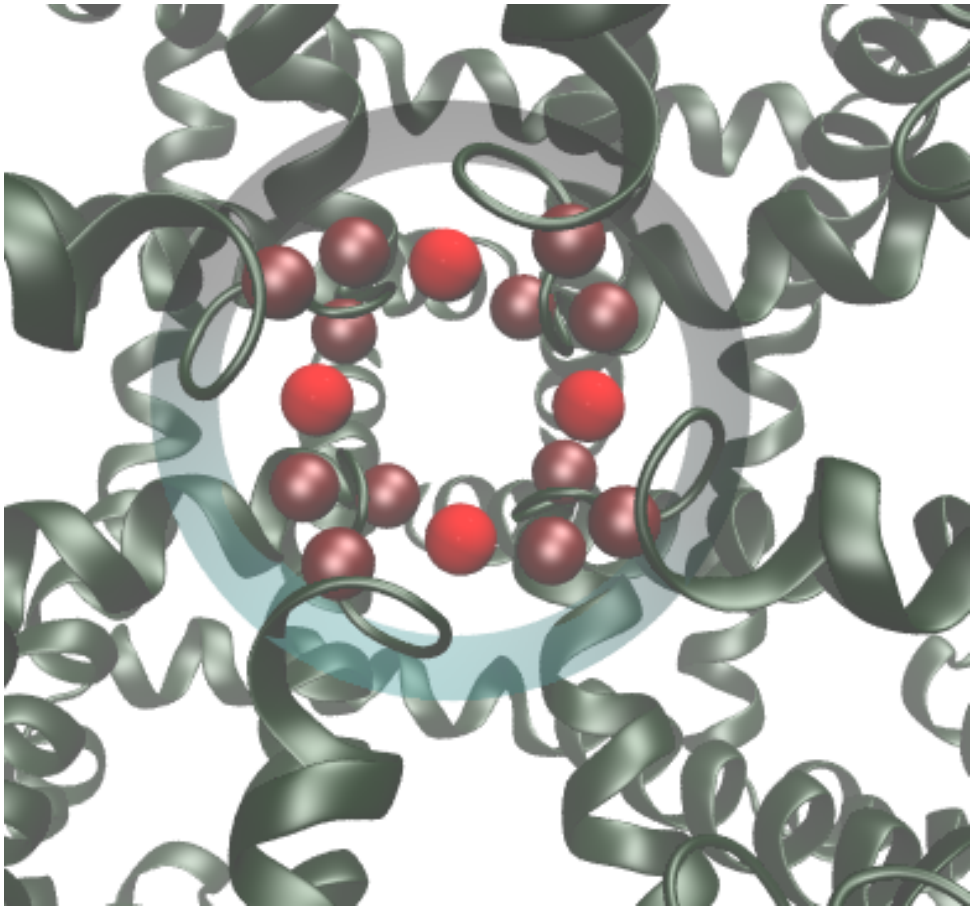

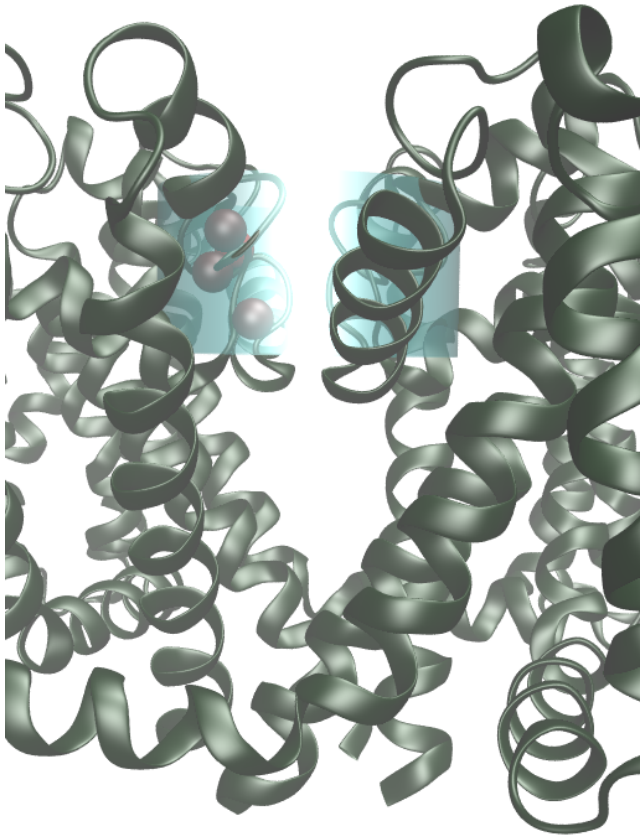

Justin Finnerty

Ca^{2+} channel: Volume model

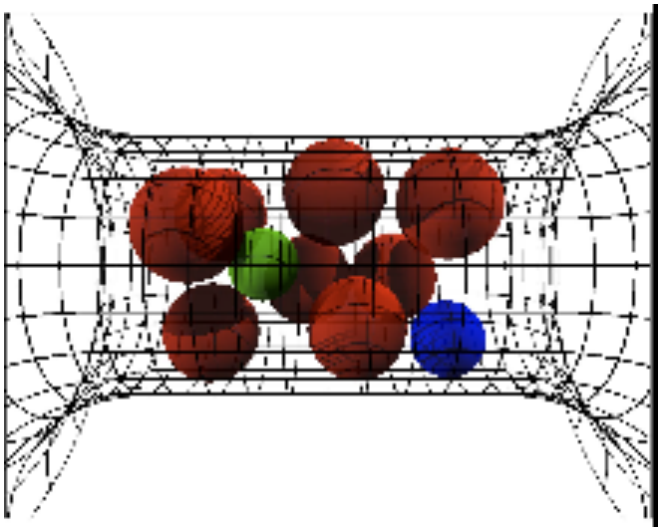

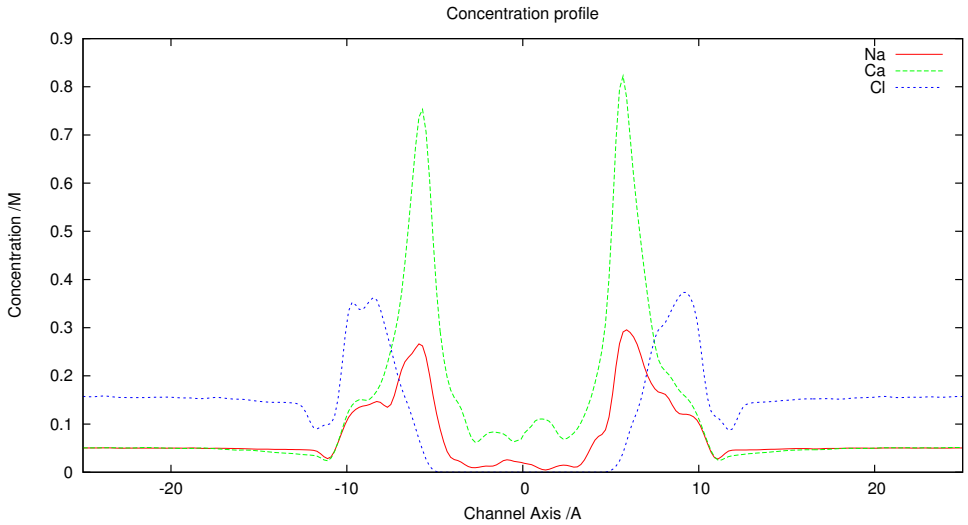

Justin Finnerty

Ca^{2+} channel: Plus dielectrics

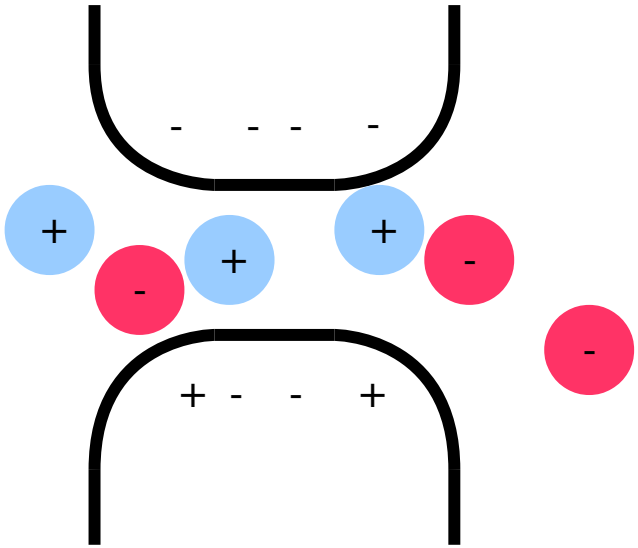

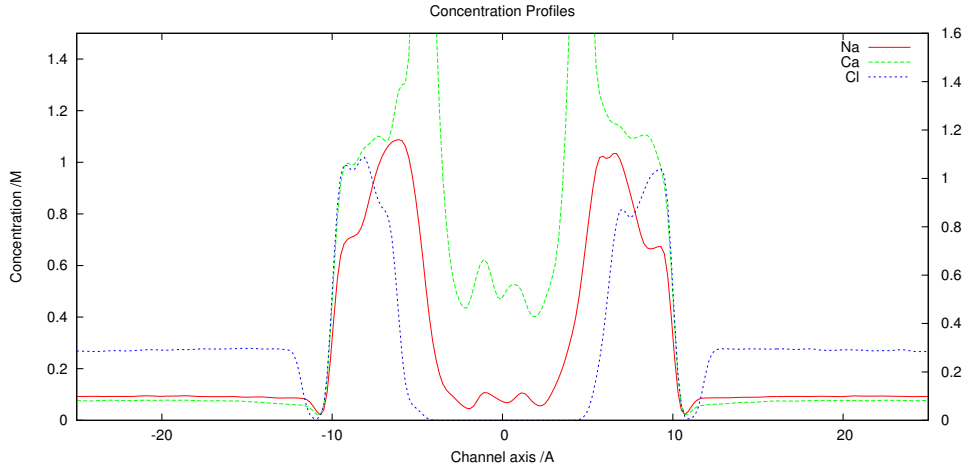

Justin Finnerty

Ca^{2+} channel: Plus localization

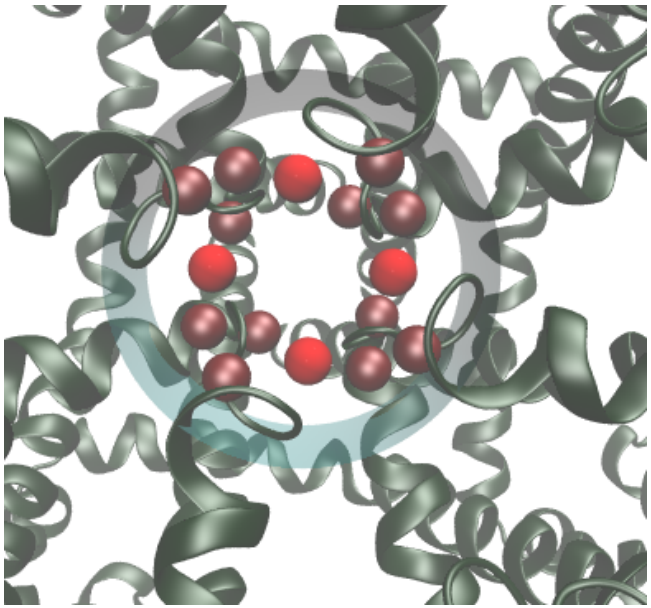

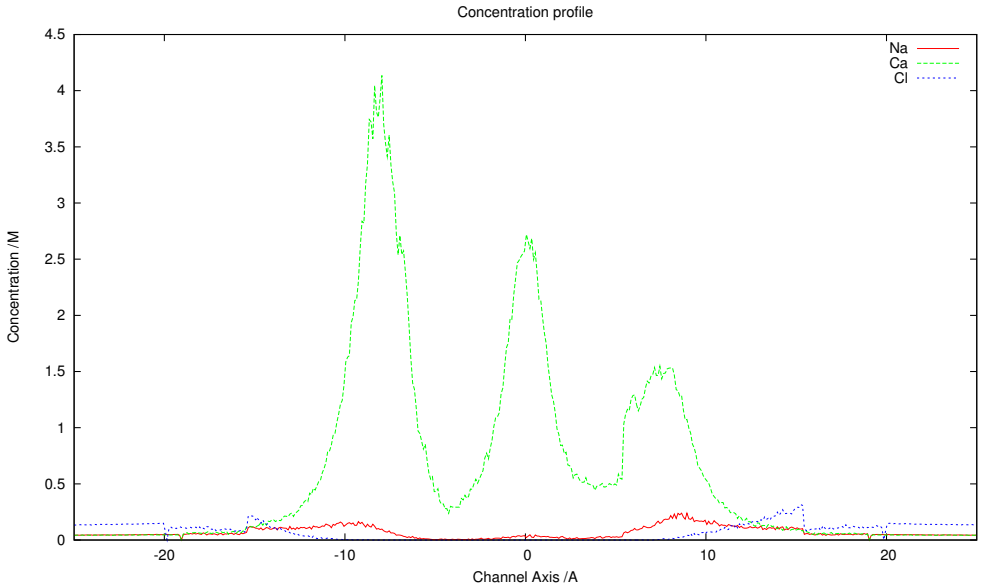

Justin Finnerty

(De)Hydration effects

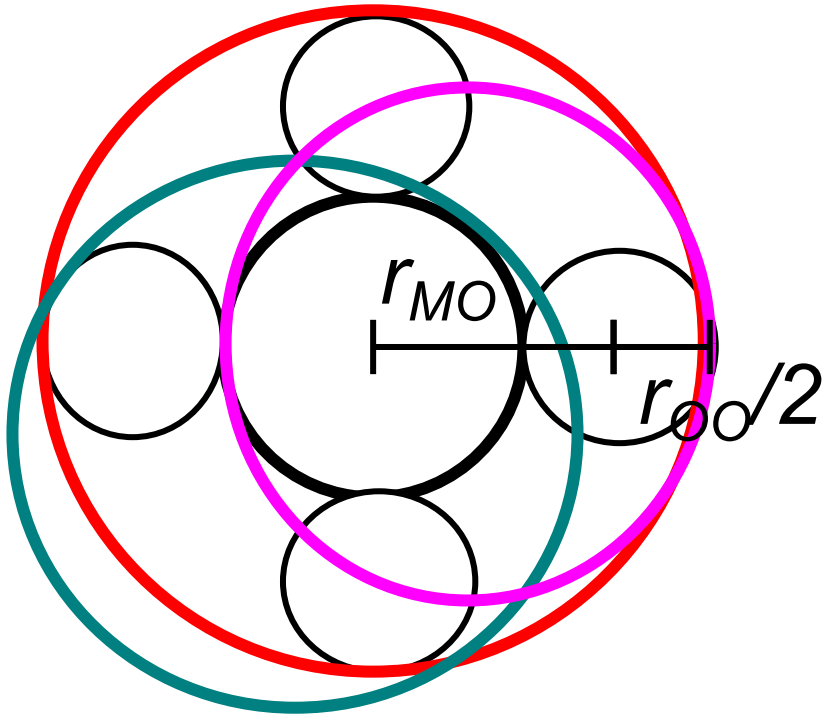

	K^+		Na^+		Ca^{2+}	
	$K_{dh(x),K^+}$	$d_{K^+,x}$	$K_{dh(x),Na^+}$	$d_{Na^+,x}$	$K_{dh(x),Ca^{2+}}$	$d_{Ca^{2+},x}$
$x = 6$	1	8.32	1	7.44	1	7.44
5	2.2×10^{-2}	$\approx$8.32	5.8×10^{-3}	$\approx$7.44	1.8×10^{-16}	$\approx$7.44
4	5.5×10^{-5}	6.21	1.7×10^{-5}	5.44	4.4×10^{-34}	5.44
3	2.5×10^{-8}	5.54	3.7×10^{-10}	5.10	8.5×10^{-53}	5.10
2	7.9×10^{-13}	2.8	6.3×10^{-17}	2.0		

(De)Hydration results

Multiple partial hydration state model

Ions A, B	Hyd.	$\frac{K_{dh(n),A}}{K_{dh(m),B}}$	K_2	α	Expt	
		KcsA Doyle et al. (1998)				
K^+,Na^+	$n, m \leq 2$	13000	0.1	1,300	> 170	LeMasurier et al. (2001)
		NavMs McCusker et al. (2012)				
Na^+,K^+	$n, m \leq 4$	0.3	30	9	11-18	Ulmschneider et al. (2013)
		NavAb Payandeh et al. (2011)				
Na^+,K^+	$n, m \leq 4$	0.3	12	2.4	6-30	Finol-Urdaneta et al. (2014)
		CavAb Tang et al. (2014)				
Ca^{2+},Na^+	$(n, m \leq 6)$	1	590	590	380	Tang et al. (2014)

$$\alpha = K_{\mathrm{A,B}} \equiv \frac{K_{dh(n),A}}{K_{dh(m),B}} K_2.$$

Implications

Reduced models

- Allow piecewise development of models
- Have (mathematically) explanatory power
- Naturally fit into multiscale models
- Can be mapped down to atomic scales

Voltage Gated K^+ Currents

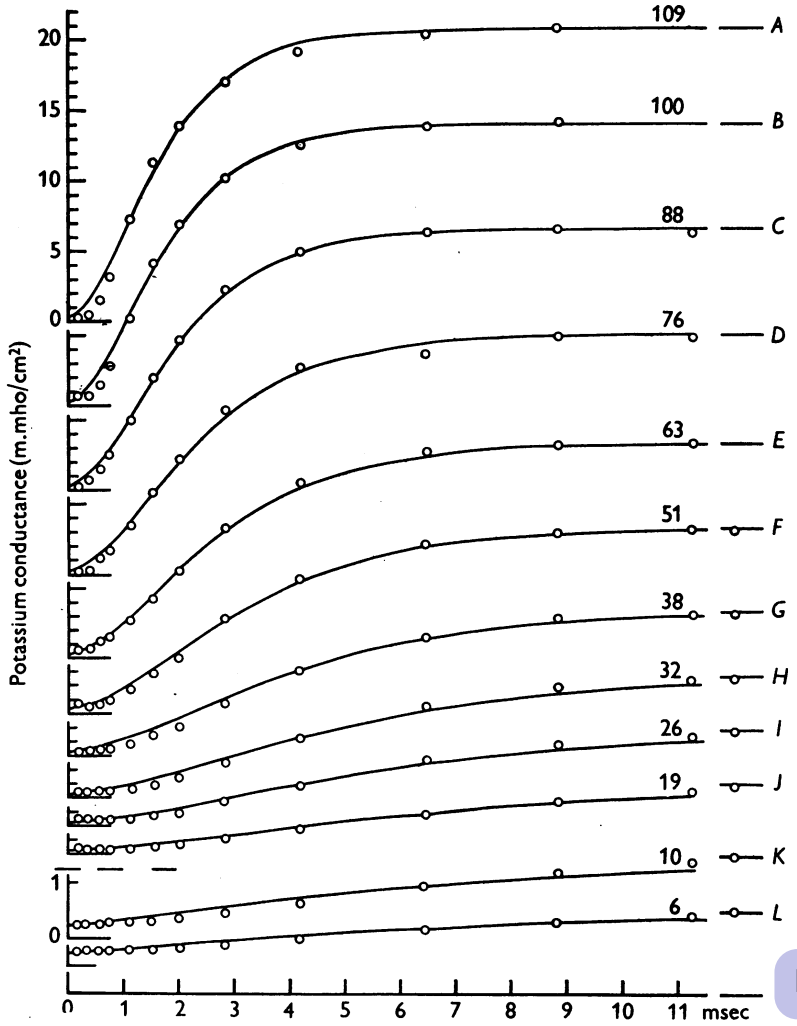

Hodgkin and Huxley (1952, Fig. 3)

$$g_K(t) = g_{K\infty}\left\{1 - \left[1 - \sqrt[4]{g_{K0}/g_{K\infty}}\right]\exp(-t/\tau_n)\right\}^4$$

Voltage-sensor displacement

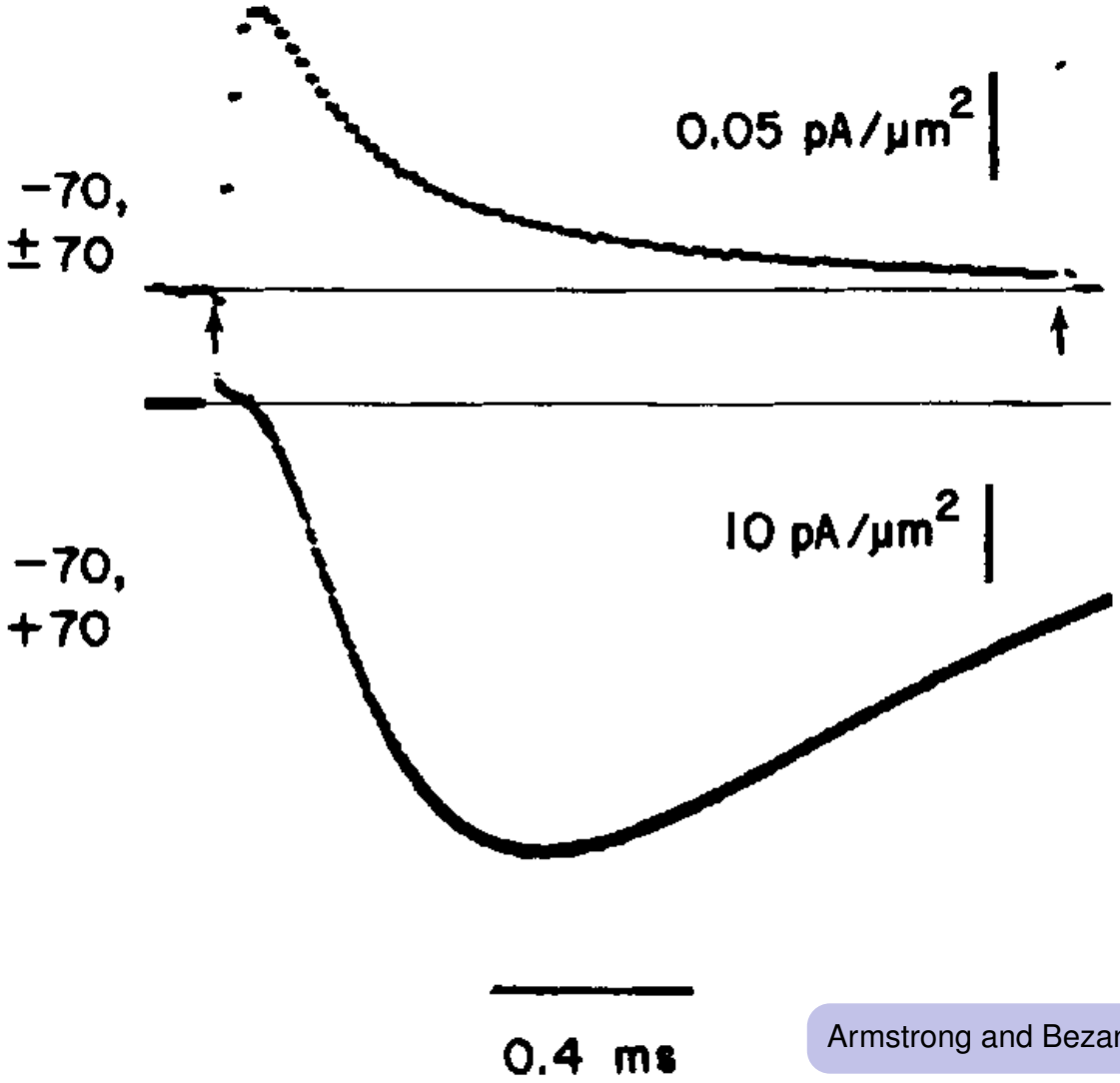

Armstrong and Bezanilla (1973, Fig. 2)

Structure

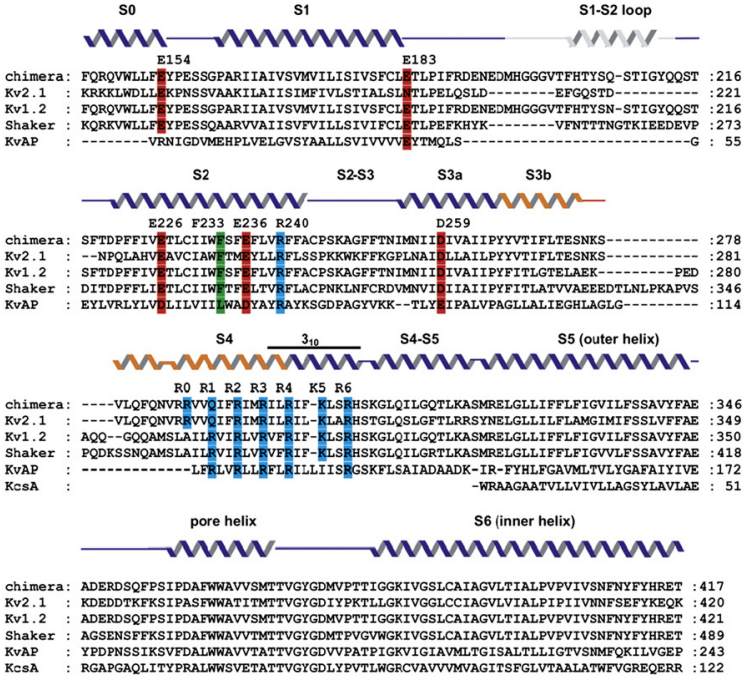

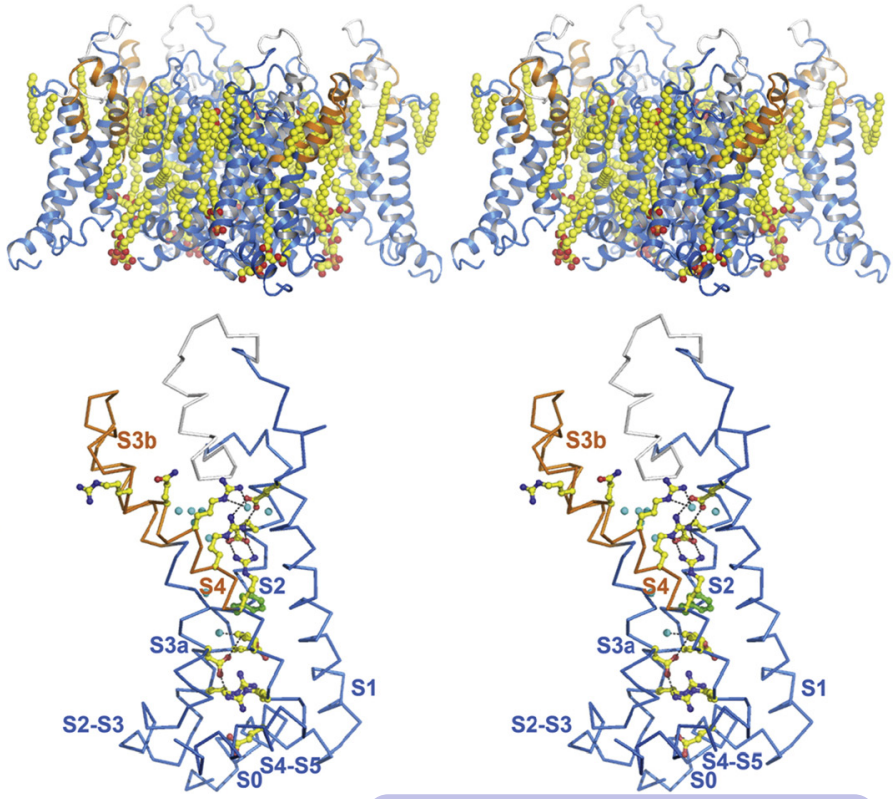

Tao and MacKinnon (2008, Fig. 1)

Geometry: Radial

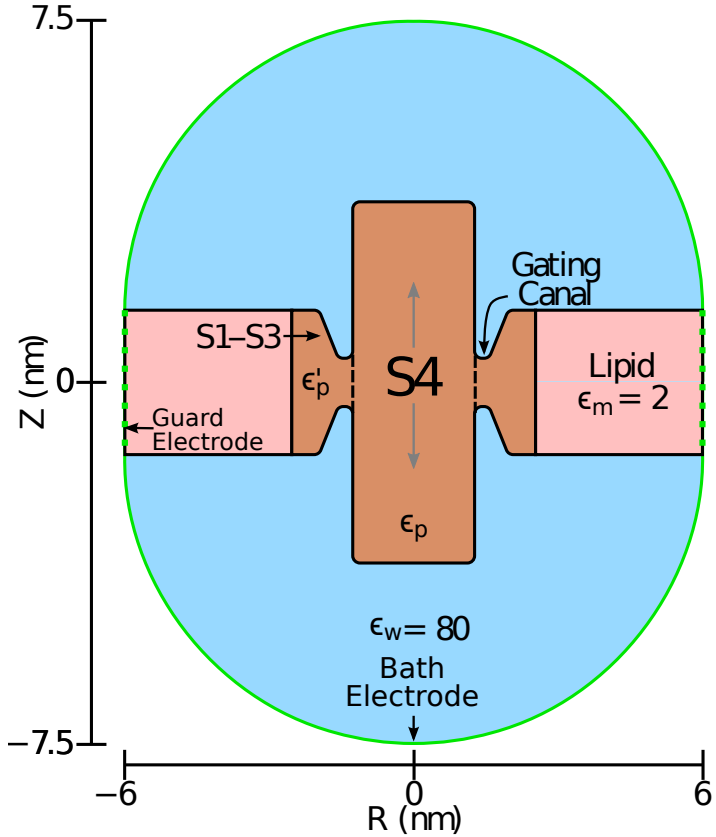

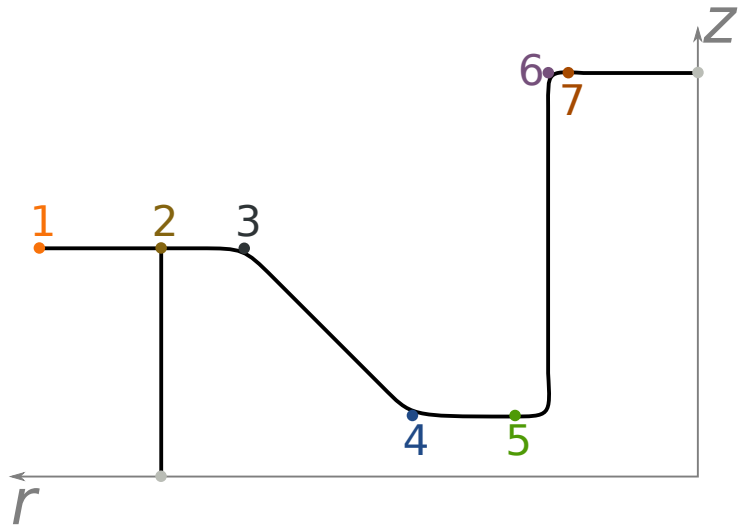

Model		1	2	3	4	5	6	7
α	r	6.0	2.532	1.966	1.566	1.466	1.266	1.0
	z	1.5	1.5	1.5	0.5015	0.5015	3.7515	3.7515
3_{10}	r	6.0	2.492	1.946	1.546	1.446	1.246	0.98
	z	1.5	1.5	1.5	0.602	0.602	4.602	4.602

Peyser and Nonner (2012a, Fig. 1)

Geometry: 3d

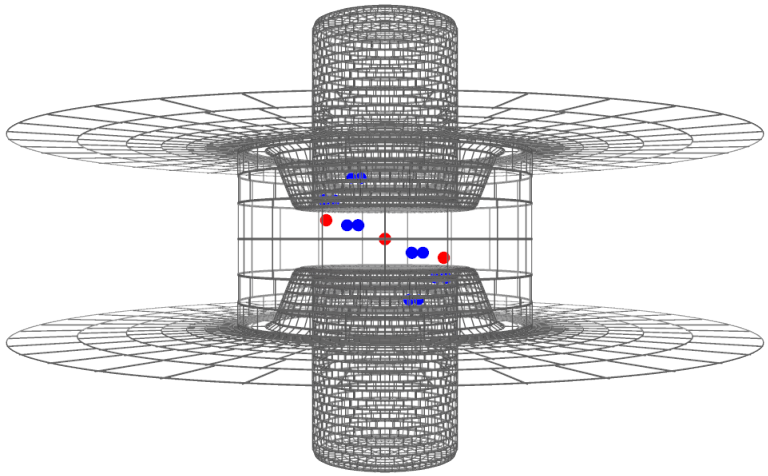

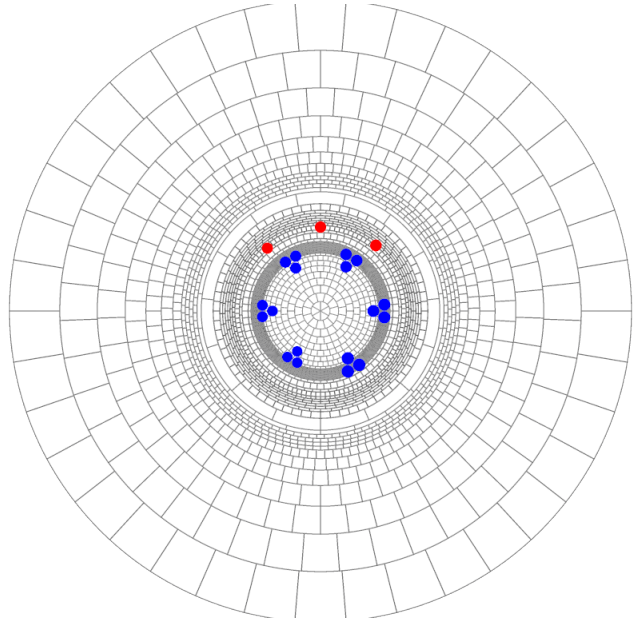

Peyser and Nonner (2012a, Fig. 2)

Single VS at 1 V: Energy & Displacement

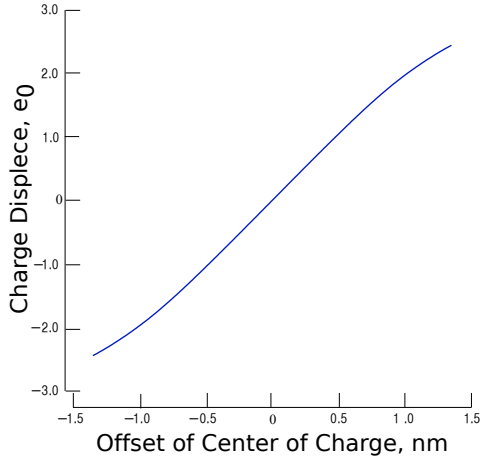

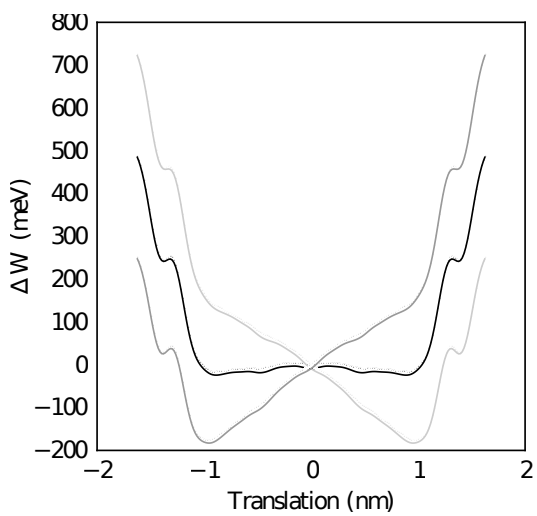

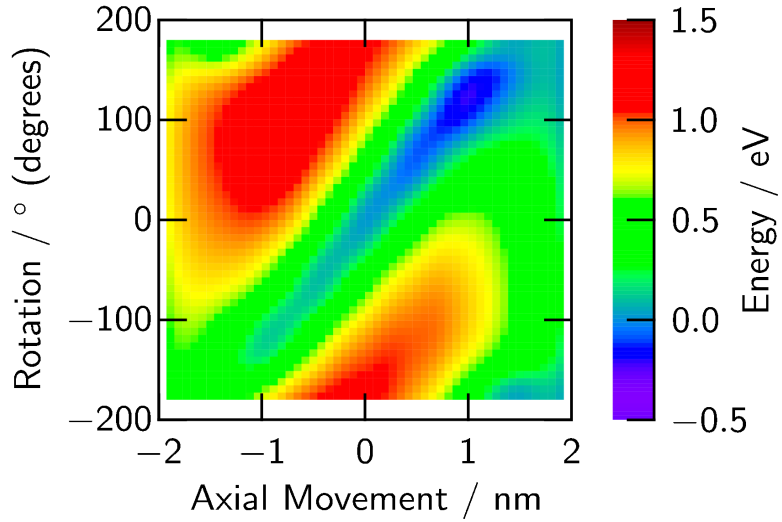

Shockley-Ramo Displacement

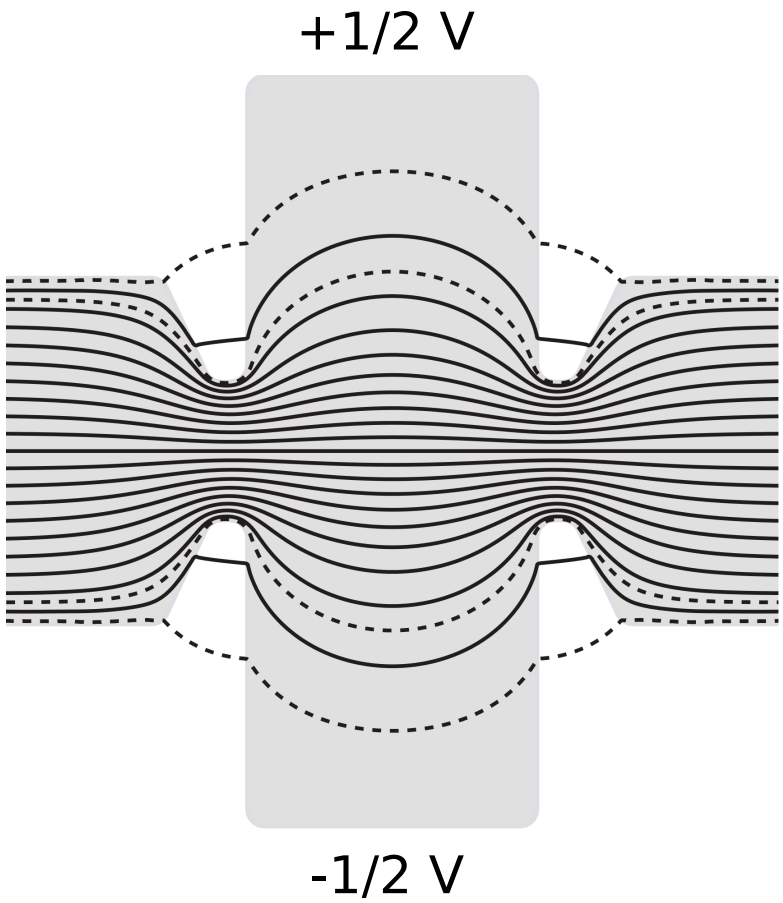

Nonner et al. (2004)

Shockley-Ramo Theorem (Integrated)

$$Q = -\sum_k q_k \; V_o(\mathbf{r}_k)/(1V)$$

Shockley-Ramo Energetics

SR can be extended to energetic calculations:

$$W = \frac{1}{2}\sum_k q_k V^{V_\varepsilon=0}(\mathbf{r}_k) - QV_m$$

All results can be calculated from one SR energy calculation with $V_m = 0$, and one SR displacement calculation $V_m = 1$ V for each conformation.

Displacement: $\langle Q \rangle$

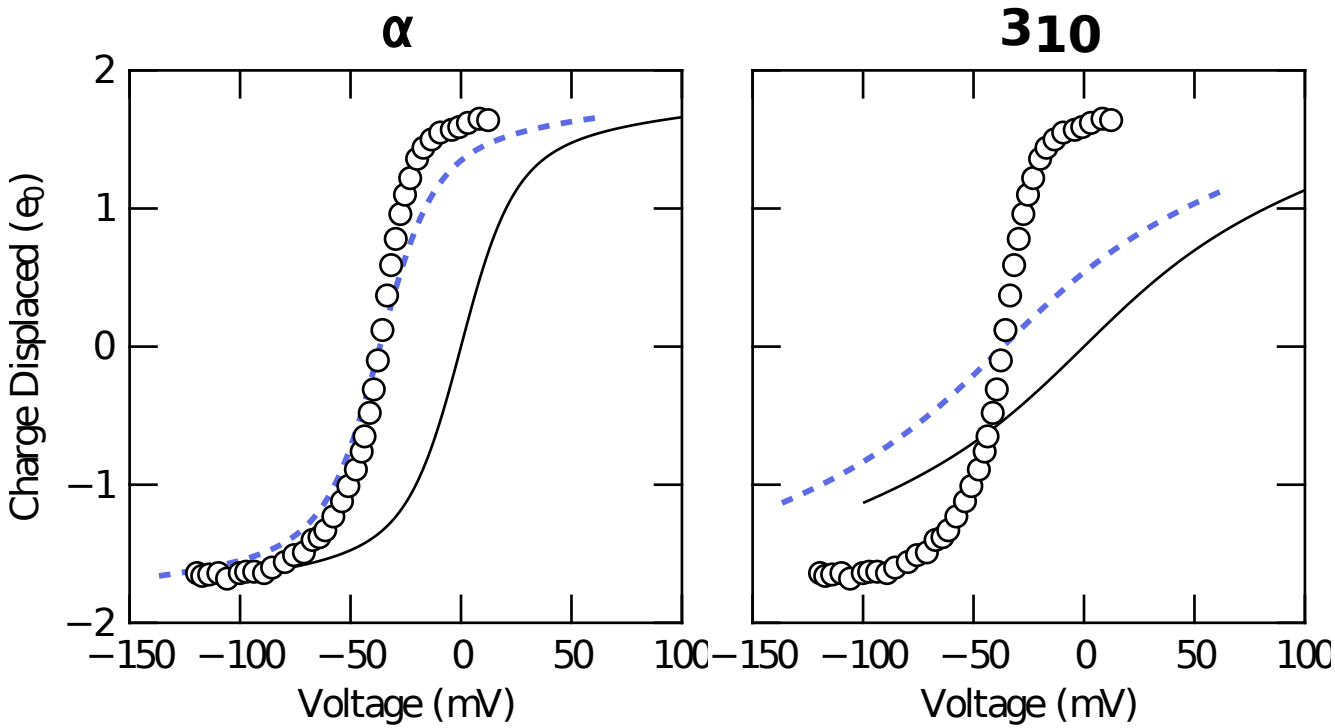

Peyser and Nonner (2012b, Fig. 3)

Seoh et al. (1996, Fig. 2)

Decomposition of a load

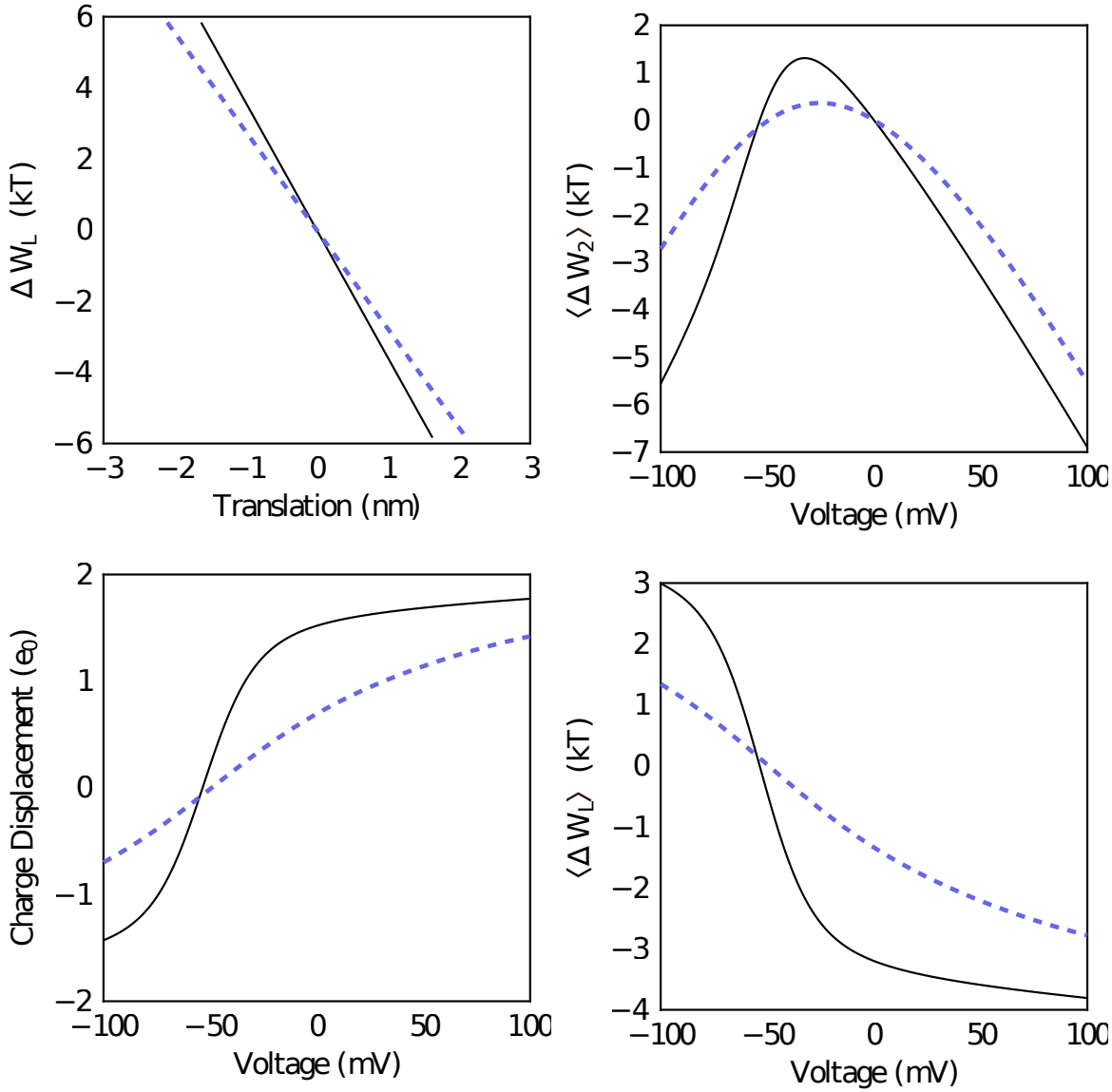

Peyser and Nonner (2012a, Fig. 8)

Multiscale gating

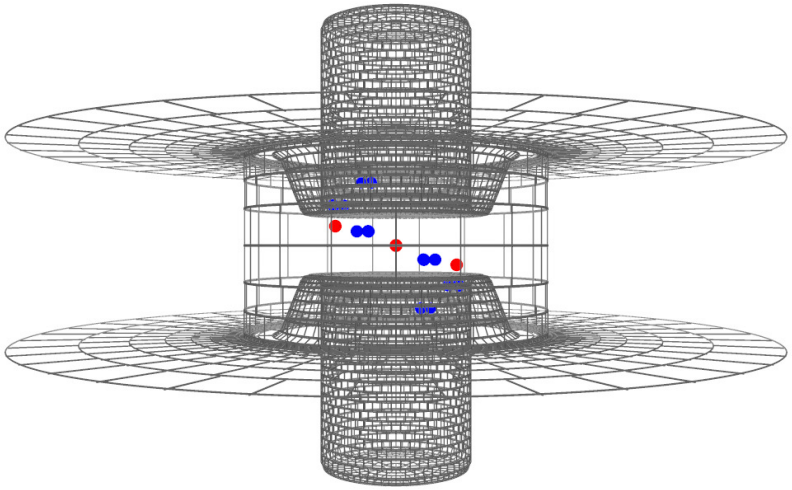

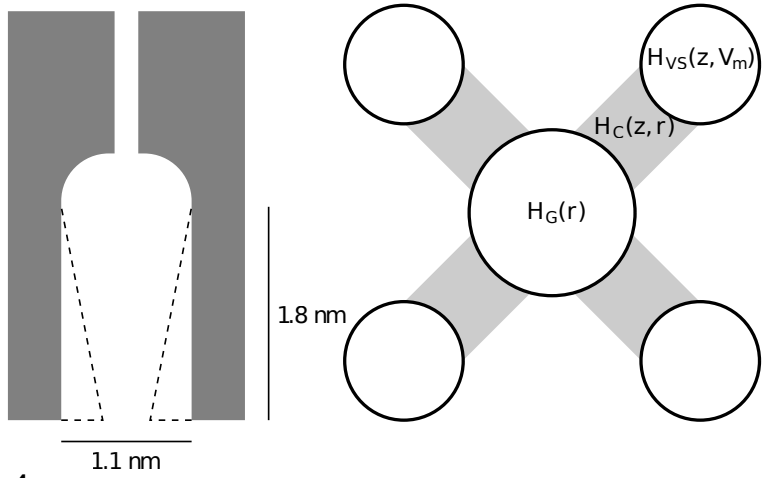

$$B(\mathbf{z}, r, V_\mathrm{m}) = \exp\{-\beta[\mathcal{H}_\mathrm{G}(r) + \sum_{i=1}^{4}(\mathcal{H}_{\mathrm{C},i}(z_i, r) + \mathcal{H}_{\mathrm{B},i}(z_i) + \mathcal{H}_{\mathrm{VS},i}(z_i, V_\mathrm{m}))]\}$$

$$\mathcal{H}_{\mathrm{VS},i}(z_i, V_\mathrm{m}) = -\beta^{-1} \ln \sum_j \exp\left[-\beta \mathcal{H}_{\mathrm{VS},i}(z_i, \phi_j, V_\mathrm{m})\right]$$

Gate model

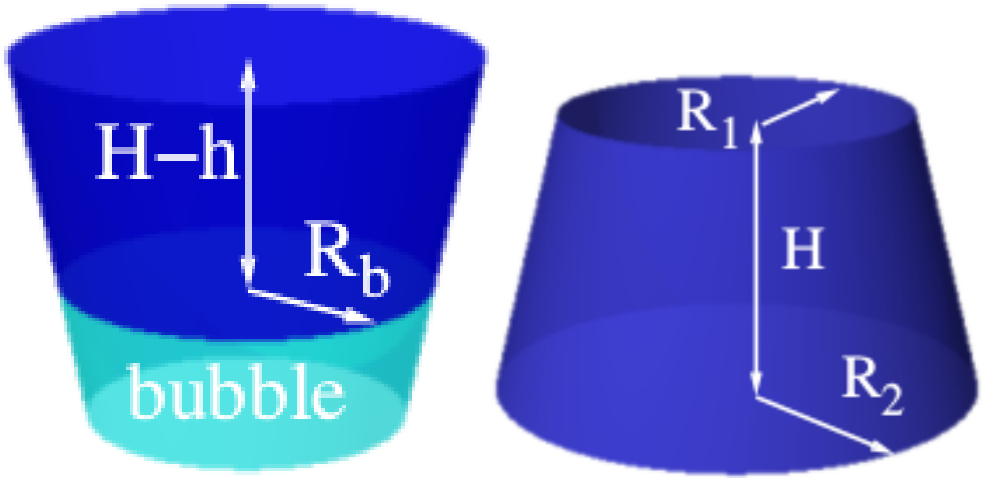

Roland Roth

$$P_{\text{open}}(R_2) = (1 + \exp(-\beta \Delta\Omega(R_2)))^{-1}$$

$$\Omega^{\text{open}}_{\text{gate}} = -p_l V(H, R_1, R_2) + \sigma_l M(H, R_1, R_2) + \kappa_l C(H, R_1, R_2)$$

$$\begin{aligned}\Omega^{\text{closed}}_{\text{gate}} = &- p_l V(H-h, R_1, R_b) + \sigma_l M(H-h, R_1, R_b) + \kappa_l C(H-h, R_1, R_b) \\ &- p_g V(h, R_b, R_2) + \sigma_g M(h, R_b, R_2) + \kappa_g C(H-h, R_b, R_2) \\ &+ \sigma_{gl}(A(R_b) + A(R_2))\end{aligned}$$

Hamiltonians & lower scale inputs

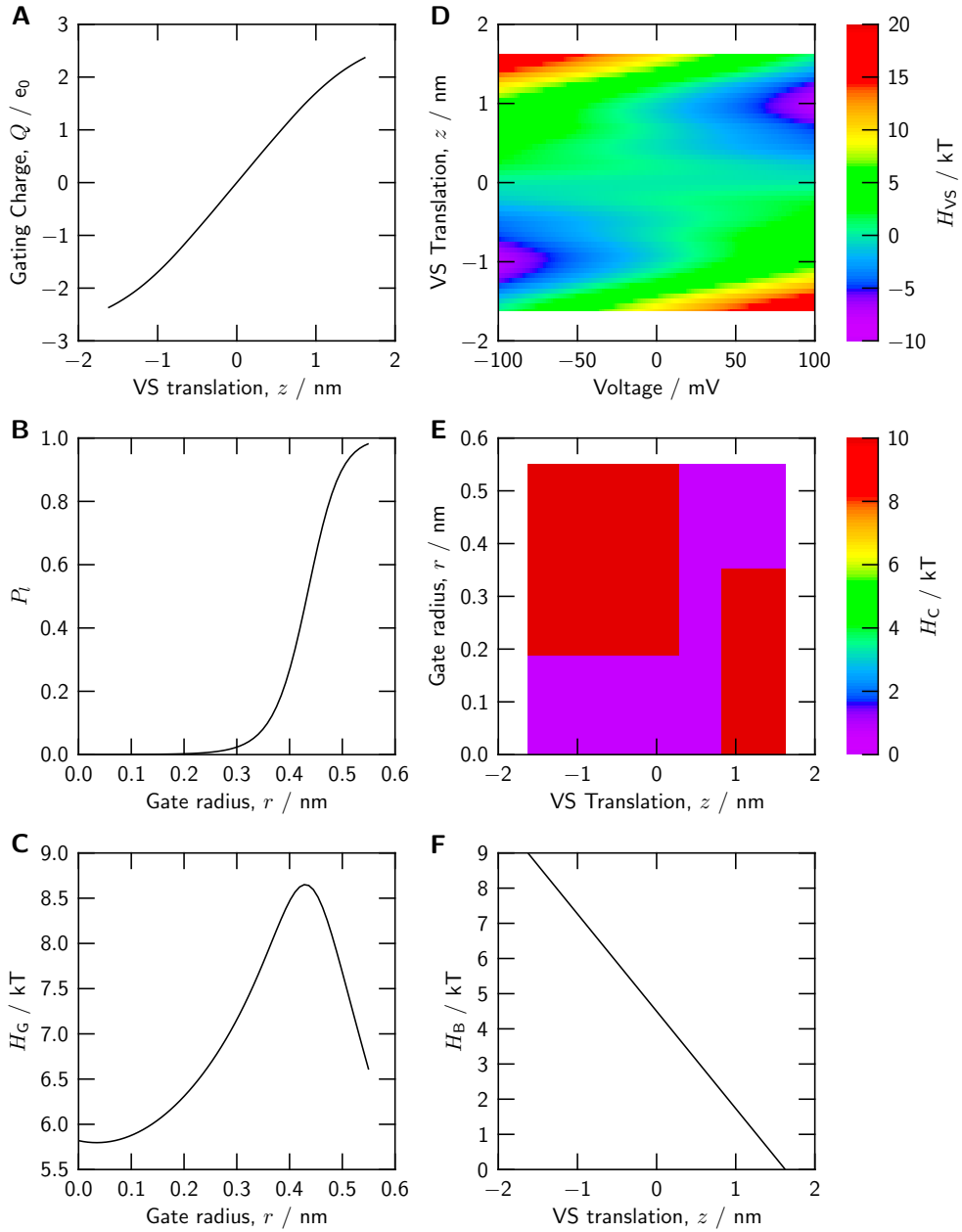

Full-channel experimental predictions

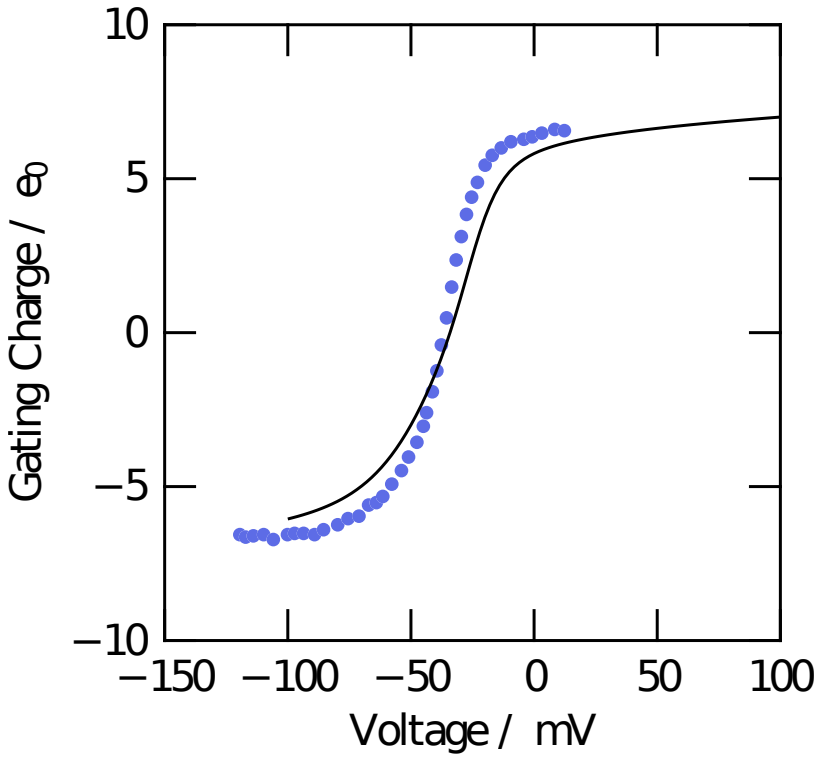

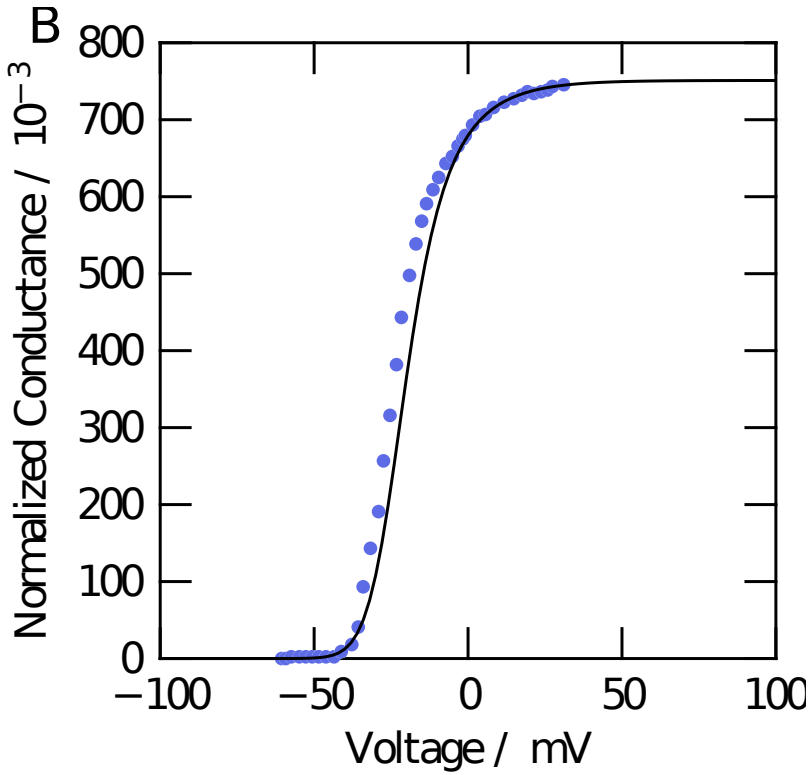

$$\mathcal{Q}(V_{\mathrm{m}}) = \sum_{l=1}^{N_r} \sum_{k_1=1}^{N_z} \sum_{k_2=k_1}^{N_z} \sum_{k_3=k_2}^{N_z} \sum_{k_4=k_3}^{N_z} n(k_1, k_2, k_3, k_4) B(z_{k_1}, z_{k_2}, z_{k_3}, z_{k_4}, r_l, V_{\mathrm{m}})$$

Mutant of first extracellular VS charge Shaker R362Q

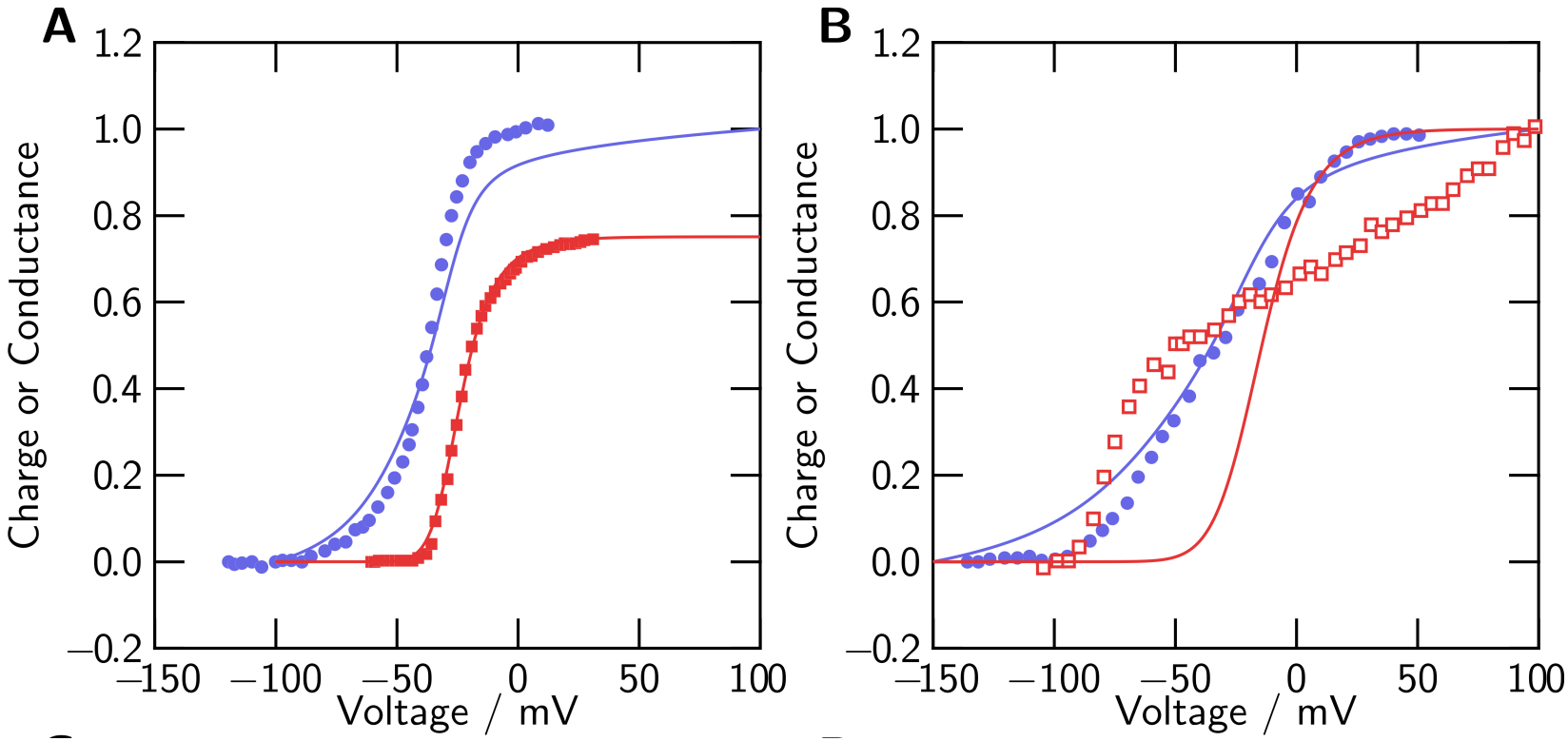

Wolfgang Nonner

Implications

Multiscale models

- Allow piecewise development of models
- Have (mathematically) explanatory power
- Decompose systems into useful subsystems
- Look like engineering descriptions
- Can combine disparate physics
- Can naturally be used to formulate falsifiable hypotheses

Overview:
Human Brain Project

JÜLICH
FORSCHUNGSZENTRUM

Boris Orth

HBP

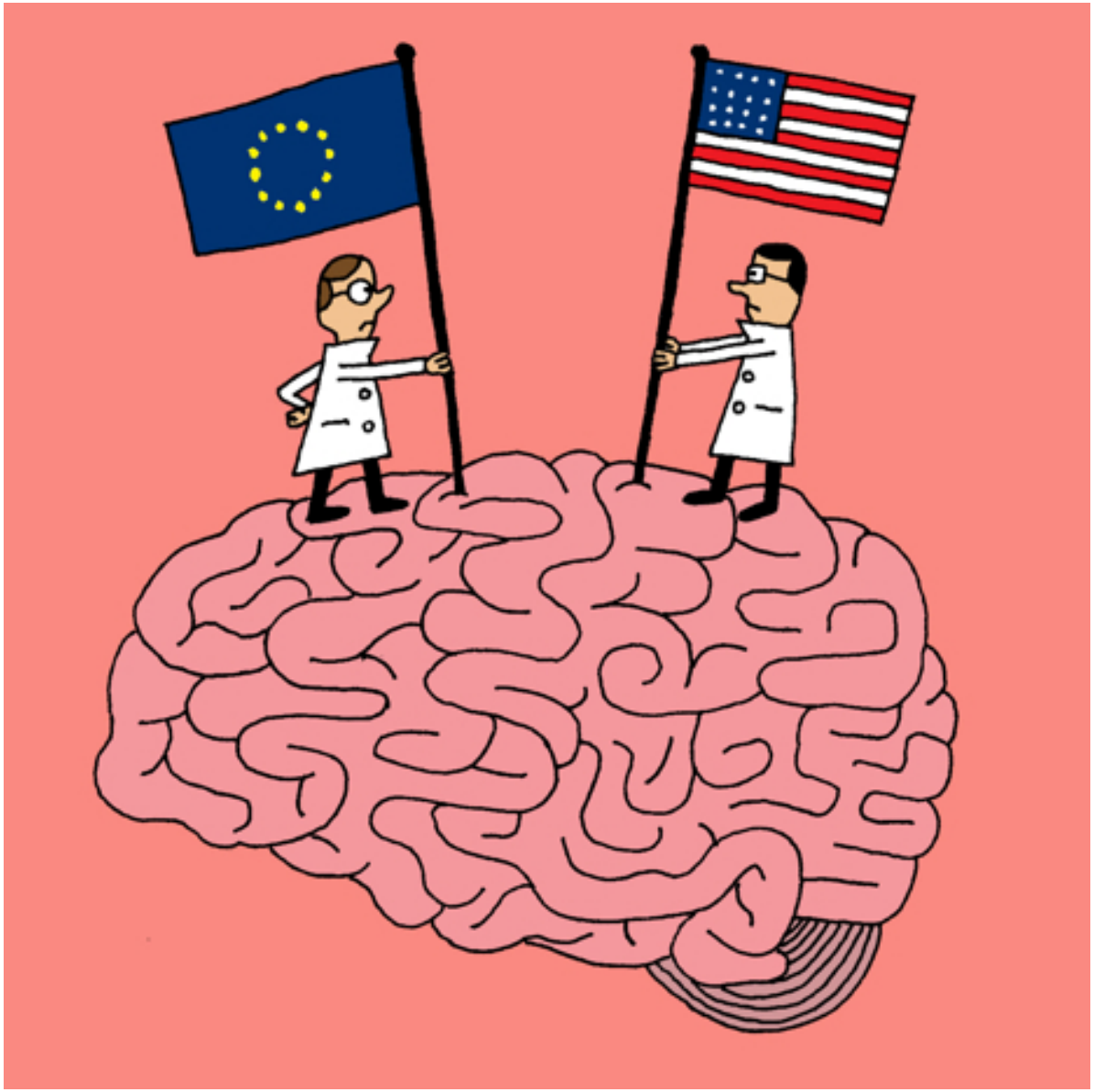

BRAIN
aka
BAM

The New Yorker
18 Feb 2013

An environment for neural systems simulations

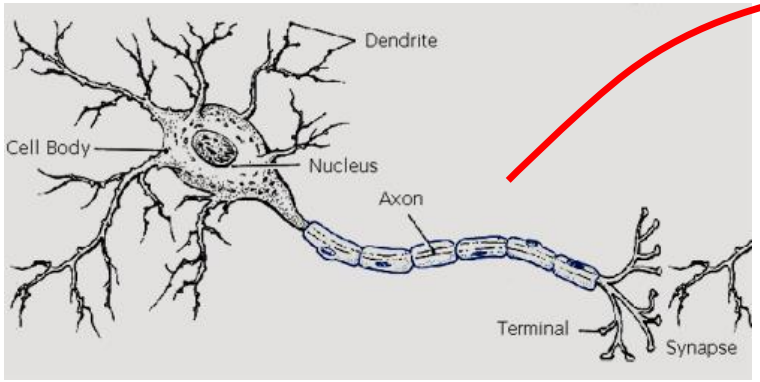

Neuron

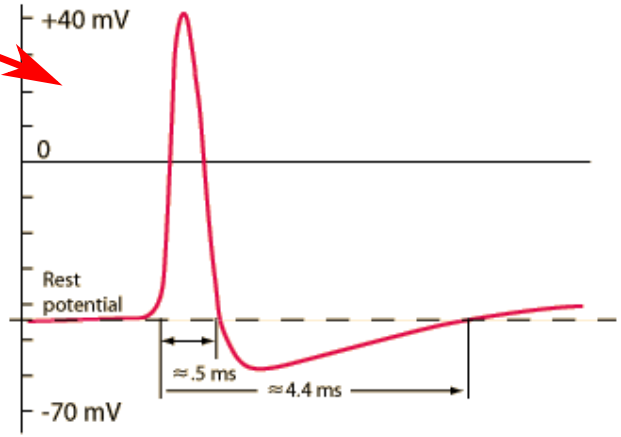

Spike

Wolfram Schenk

$$dV/dt = (-V + IR_m)/\tau_m$$

An environment for neural systems simulations

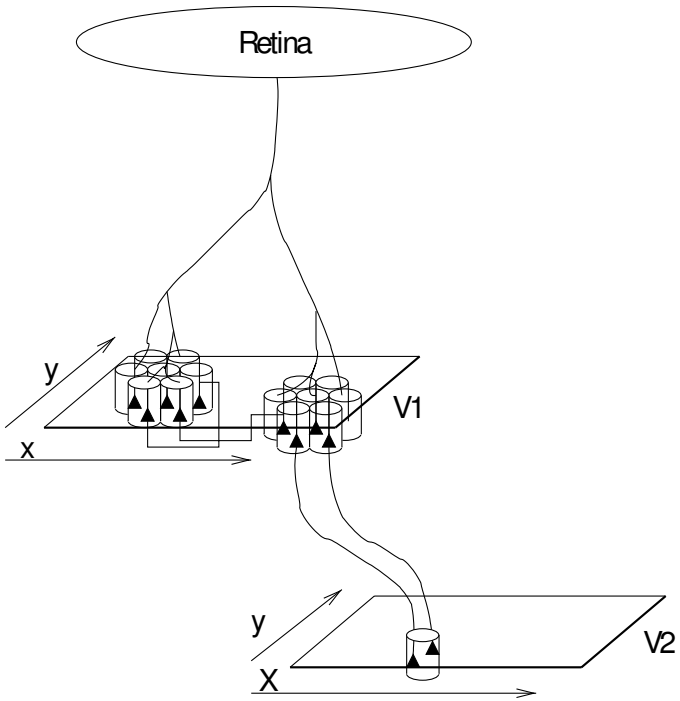

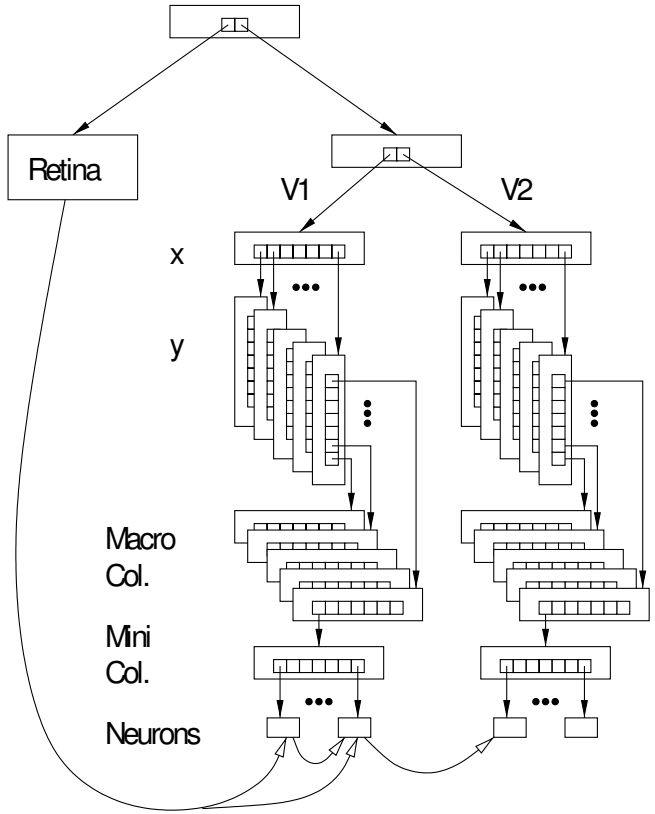

Diesmann and Gewaltig (2001)

Short term plasticity

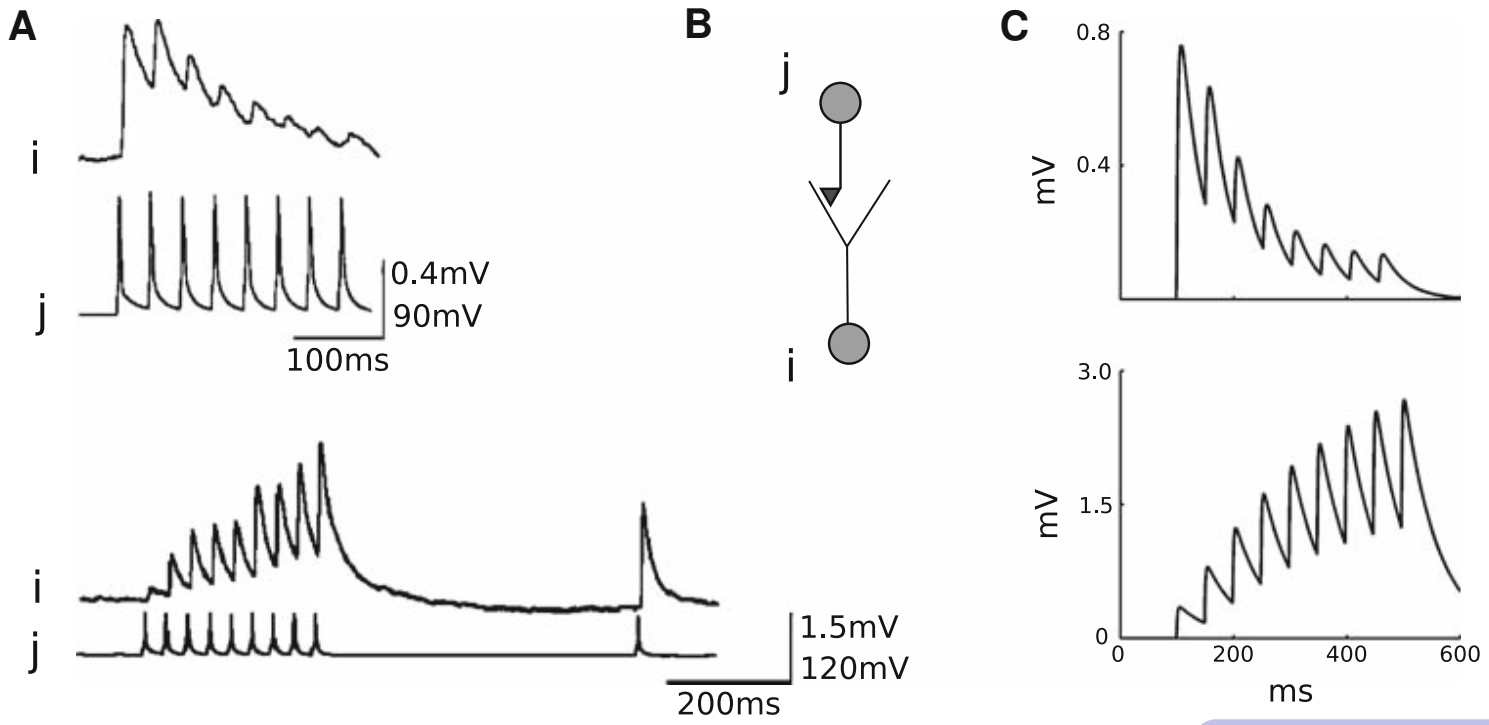

Morrison et al. (2008, Fig. 2)

$$dx/dt = z/\tau_{rec} - u_+ x - \delta(t - t_j^f)$$

$$dy/dt = -y/\tau_I + u_+ x - \delta(t - t_j^f)$$

$$dz/dt = y/\tau_I - z/\tau_{rec}$$

Long term plasticity

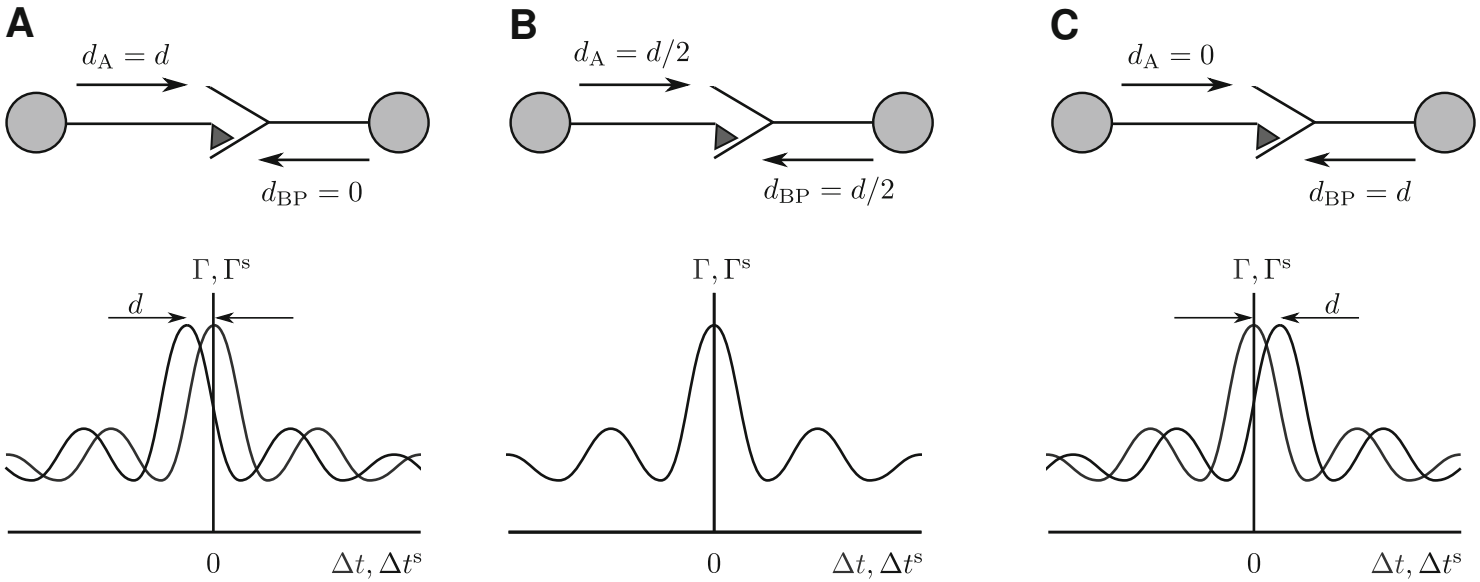

Morrison et al. (2008, Fig. 8)

$$\dot{w} = -F_-(w) \int_{-\infty}^{0} d\Delta t^s \; K_-(\Delta t^s)\, \Gamma(\Delta t^s + (d_A - d_{BP}))$$
$$+ F_+(w) \int_{0}^{\infty} d\Delta t^s \; K_+(\Delta t^s)\, \Gamma(\Delta t^s + (d_A - d_{BP}))$$

Microcircuit model

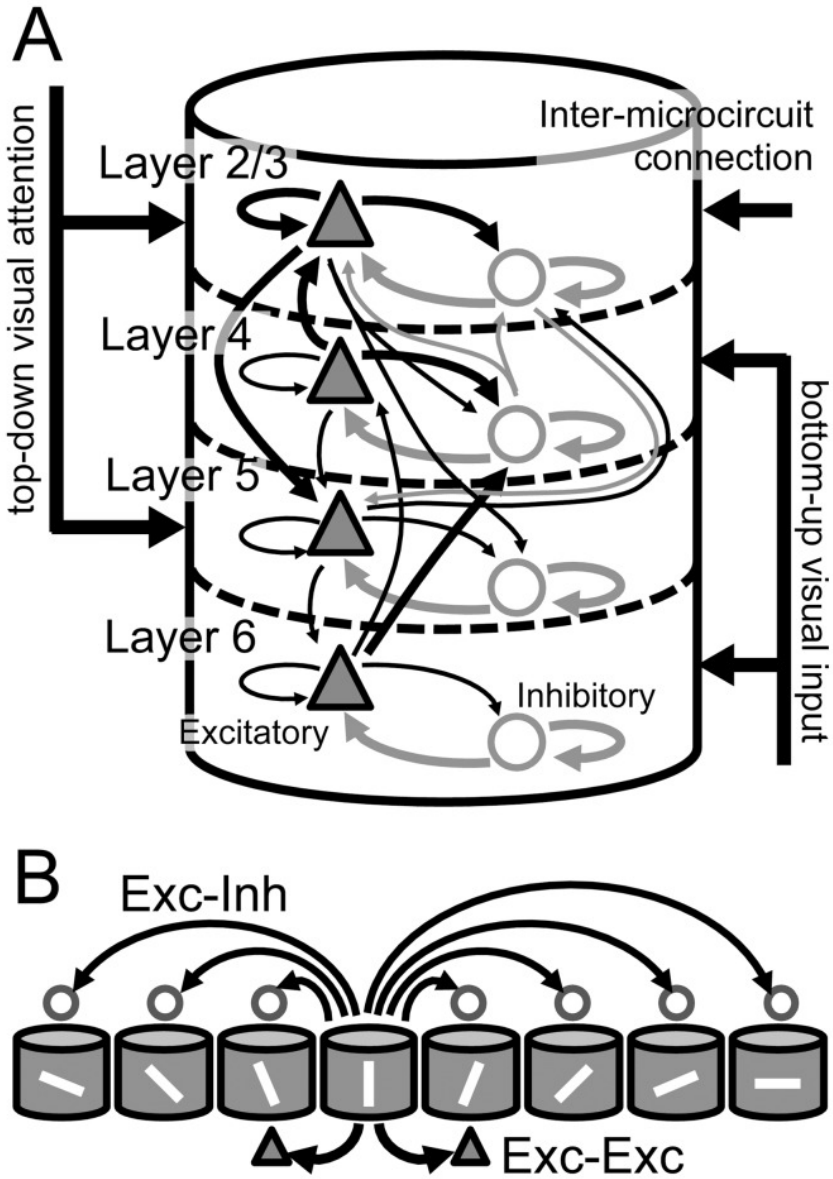

Wagatsuma et al. (2013)

VisNest: Connecting multiple centers

Christian Nowke

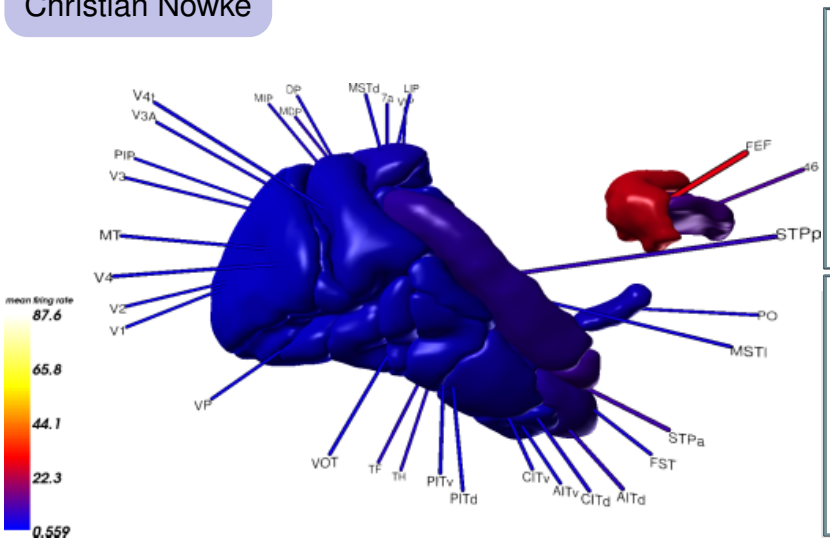

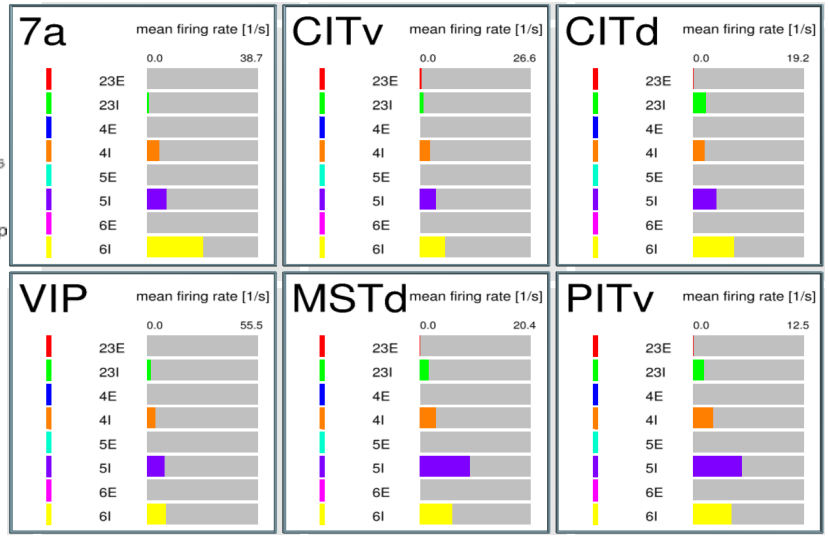

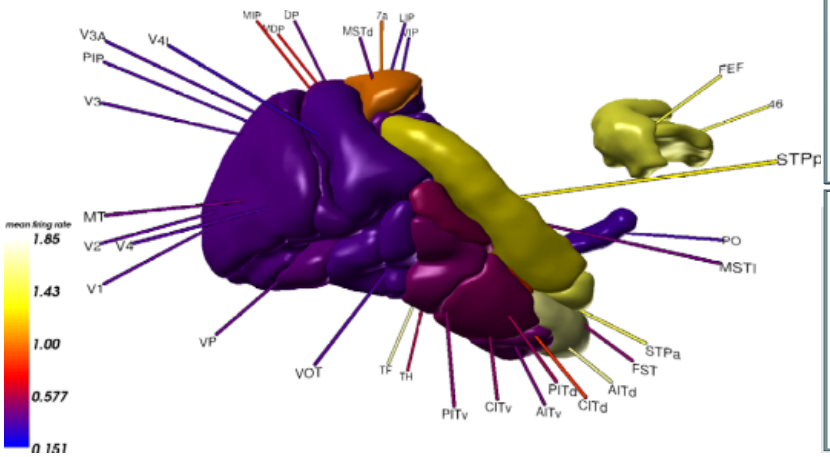

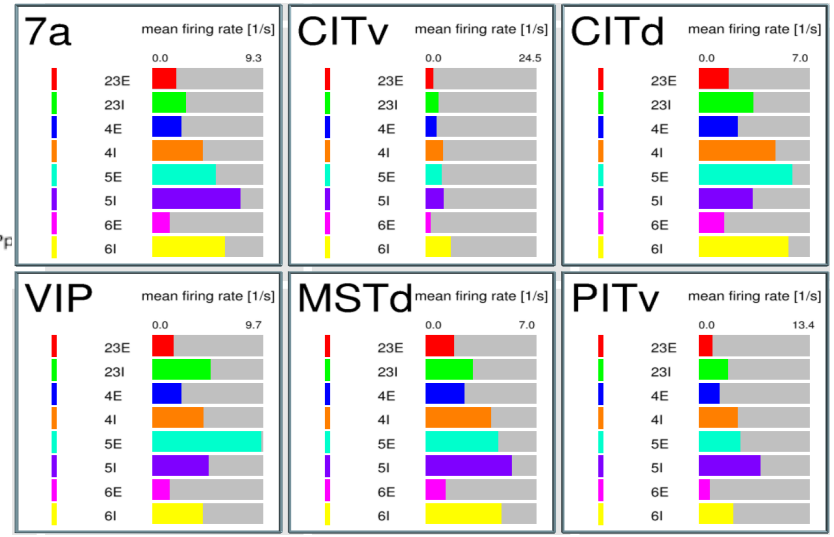

The gap between molecular models and tissues

From subcellular to supercellular

Neuron	is the major project within the HBP modeling neurons at the cable compartment level
Subcellular	projects are still in early stages, such as electrically accurate synapse models
Supracellular	projects tend to be highly reduced, but are being developed for cardiac and hepatic systems in addition to the brain
Which How	elements should be studied at each scale and to properly link different scales are questions that are often not answered robustly

This gap is not just a problem of computational tractability, but even more importantly, one of correctness.

Acknowledgments

HPC in Neuroscience

Boris Orth
Andrew Adinetz
Martin Stöckle
Bastian Tweddell
Anne Do Lam-Ruschewski

RWTH Aachen University

Christian Nowke

German Research School for Simulation Sciences

Justin Finnerty
Emiliano Ippoliti

SimLab Neuroscience

Abigail Morrison
Rajalekshmi Deepu
Mikaël Naveau
Yury Zaytsev
Wolfram Schenck
Anna Lührs
Sven Strohmer
Susanne Kunkel
Markus Butz-Ostendorf

University of Miami

Wolfgang Nonner
Karl Magleby
Alice Holohean

Rush University

Bob Eisenberg
Dirk Gillespie

Universität Tübingen

Roland Roth

University of Florence

Claudio Luchinat
Enrico Ravera
Giacomo Parigi

Funding

Deutsche Forschungsgemeinschaft
Helmholtz Association:
SMBH: Supercomputing and Modelling for Human Brain
JARA: Jülich Aachen Research Alliance
University of Miami
National Institutes of Health
NSF Graduate Research Fellowship
German Research School for Simulation Sciences

Any opinions, findings, conclusions or recommendations expressed in this publication are those of the author and do not necessarily reflect the views of any funders.

References I

C. Armstrong and F. Bezanilla. Currents related to movement of the gating particles of the sodium channels. Nature, 242(5398):459–461, 13 Apr. 1973. doi: 10.1038/242459a0.

M. Diesmann and M.-O. Gewaltig. NEST: An environment for neural systems simulations. Forschung und wisschenschaftliches Rechnen, 58:43–70, 2001.

D. A. Doyle, J. M. Cabral, R. A. Pfuetzner, A. Kuo, J. M. Gulbis, S. L. Cohen, B. T. Chait, and R. MacKinnon. The structure of the potassium channel: molecular basis of k+ conduction and selectivity. Science, 280(5360):69–77, Apr 1998.

R. K. Finol-Urdaneta, Y. Wang, A. Al-Sabi, C. Zhao, S. Y. Noskov, and R. J. French. Sodium channel selectivity and conduction: Prokaryotes have devised their own molecular strategy. The Journal of General Physiology, 143(2):157–171, 2014. doi: 10.1085/jgp.201311037.

References II

A. Hodgkin and A. Huxley. A quantitative description of membrane current and its application to conduction and excitation in nerve. J Physiol, 117(4):500–544, 1952. ISSN 00223751. URL http://www.ncbi.nlm.nih.gov/pmc/articles/PMC1392413.

M. LeMasurier, L. Heginbotham, and C. Miller. KcsA: It's a potassium channels. The Journal of General Physiology, 118(3):303–314, 2001. doi: 10.1085/jgp.118.3.303.

E. C. McCusker, C. Bagnéris, C. E. Naylor, A. R. Cole, N. D'Avanzo, C. G. Nichols, and B. A. Wallace. Structure of a bacterial voltage-gated sodium channel pore reveals mechanisms of opening and closing. Nat Commun, 3:1102–, Oct. 2012. URL http://dx.doi.org/10.1038/ncomms2077.

A. Morrison, M. Diesmann, and W. Gerstner. Phenomenological models of synaptic plasticity based on spike timing. Biological Cybernetics, 98(6):459–478, 2008. ISSN 0340-1200. doi: 10.1007/s00422-008-0233-1.

References III

W. Nonner, A. Peyser, D. Gillespie, and B. Eisenberg. Relating microscopic charge movement to macroscopic currents: The Ramo-Shockley theorem applied to ion channels. Biophys J, 87(6): 3716–3722, 2004. ISSN 0006-3495.
doi: http://dx.doi.org/10.1529/biophysj.104.047548.

J. Payandeh, T. Scheuer, N. Zheng, and W. A. Catterall. The crystal structure of a voltage-gated sodium channel. Nature, 475:353–358, 2011.

A. Peyser and W. Nonner. Voltage sensing in ion channels: Mesoscale simulations of biological devices. Phys Rev E Stat Nonlin Soft Matter Phys, 86:011910, July 2012a. doi: 10.1103/PhysRevE.86.011910.

A. Peyser and W. Nonner. The sliding-helix voltage sensor: mesoscale views of a robust structure-function relationship. Eur Biophys J, 41: 705–721, 2012b. ISSN 0175-7571.
doi: 10.1007/s00249-012-0847-z.

References IV

S.-A. Seoh, D. Sigg, D. M. Papazian, and F. Bezanilla. Voltage-sensing residues in the S2 and S4 segments of the Shaker K^+ channel. Neuron, 16(6):1159–1167, 1 June 1996. ISSN 0896-6273. doi: 10.1016/S0896-6273(00)80142-7.

L. Tang, T. M. Gamal El-Din, J. Payandeh, G. Q. Martinez, T. M. Heard, T. Scheuer, N. Zheng, and W. A. Catterall. Structural basis for ca^{2+} selectivity of a voltage-gated calcium channel. Nature, 505(7481): 56–61, Jan. 2014. ISSN 0028-0836. URL http://dx.doi.org/10.1038/nature12775.

X. Tao and R. MacKinnon. Functional analysis of Kv1.2 and paddle chimera Kv channels in planar lipid bilayers. J Mol Biol, 382(1):24–33, Sept. 2008. doi: 10.1016/j.jmb.2008.06.085.

References V

M. B. Ulmschneider, C. Bagnéris, E. C. McCusker, P. G. DeCaen, M. Delling, D. E. Clapham, J. P. Ulmschneider, and B. A. Wallace. Molecular dynamics of ion transport through the open conformation of a bacterial voltage-gated sodium channel. Proceedings of the National Academy of Sciences, 110(16):6364–6369, 2013. doi: 10.1073/pnas.1214667110.

N. Wagatsuma, T. C. Potjans, M. Diesmann, K. Sakai, and T. Fukai. Spatial and feature-based attention in a layered cortical microcircuit model. PLoS ONE, 8(12):e80788, 12 2013. doi: 10.1371/journal.pone.0080788.

PCS Results

Tb^{3+}

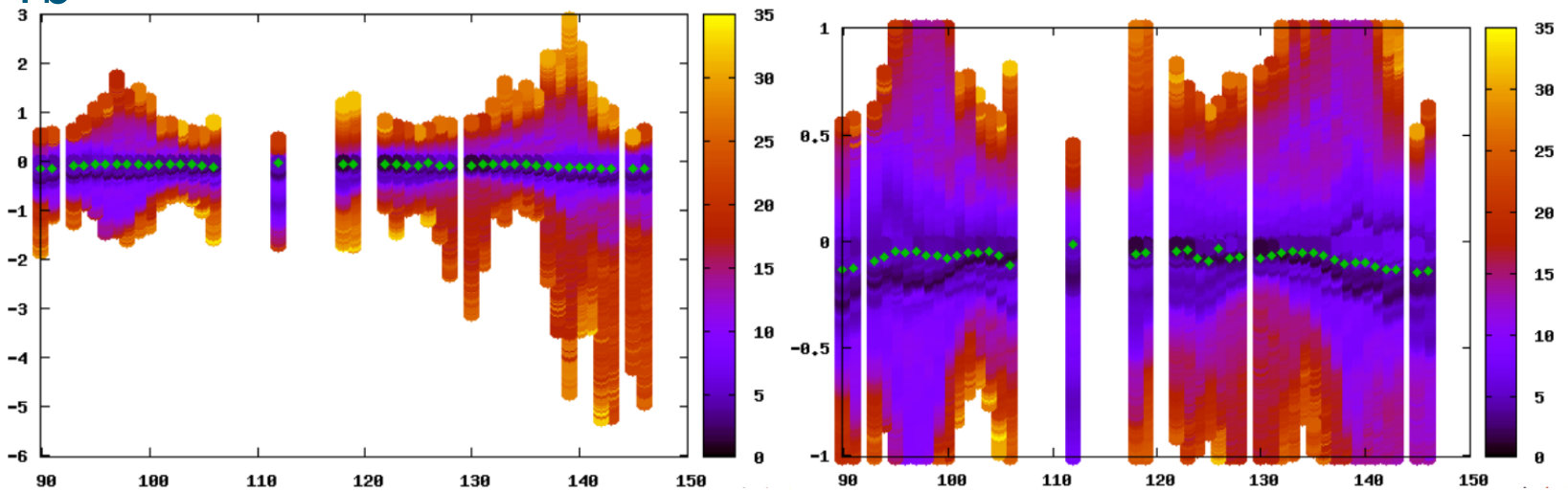

PCS Results

Tm^{3+}

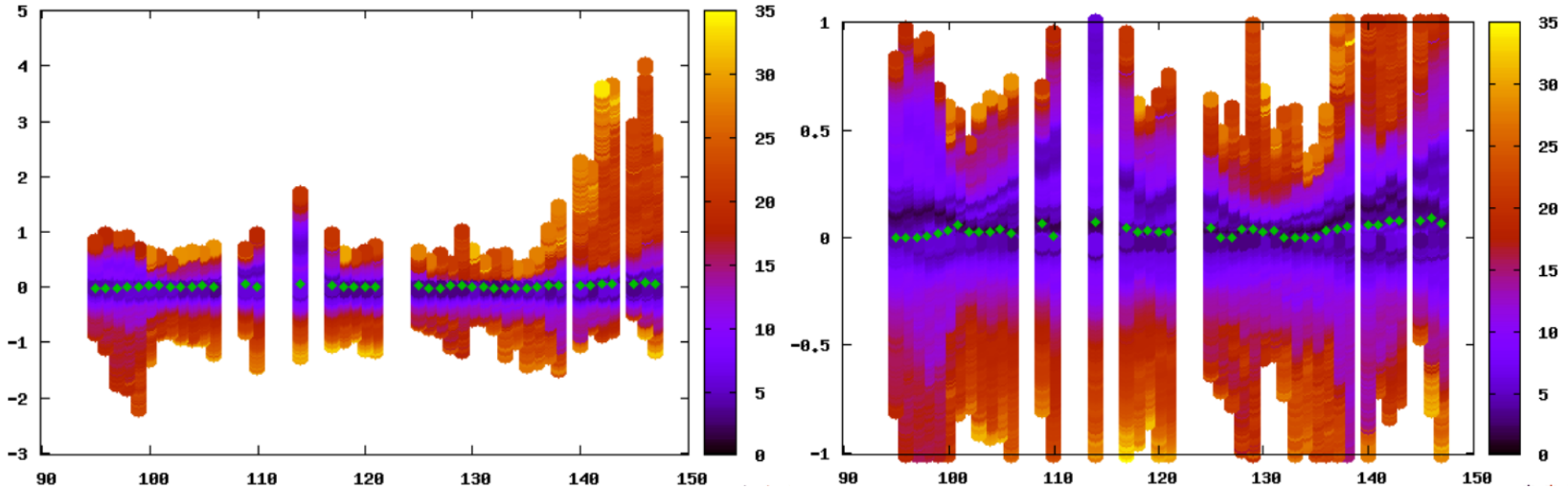

PCS Results

Dy^{3+}

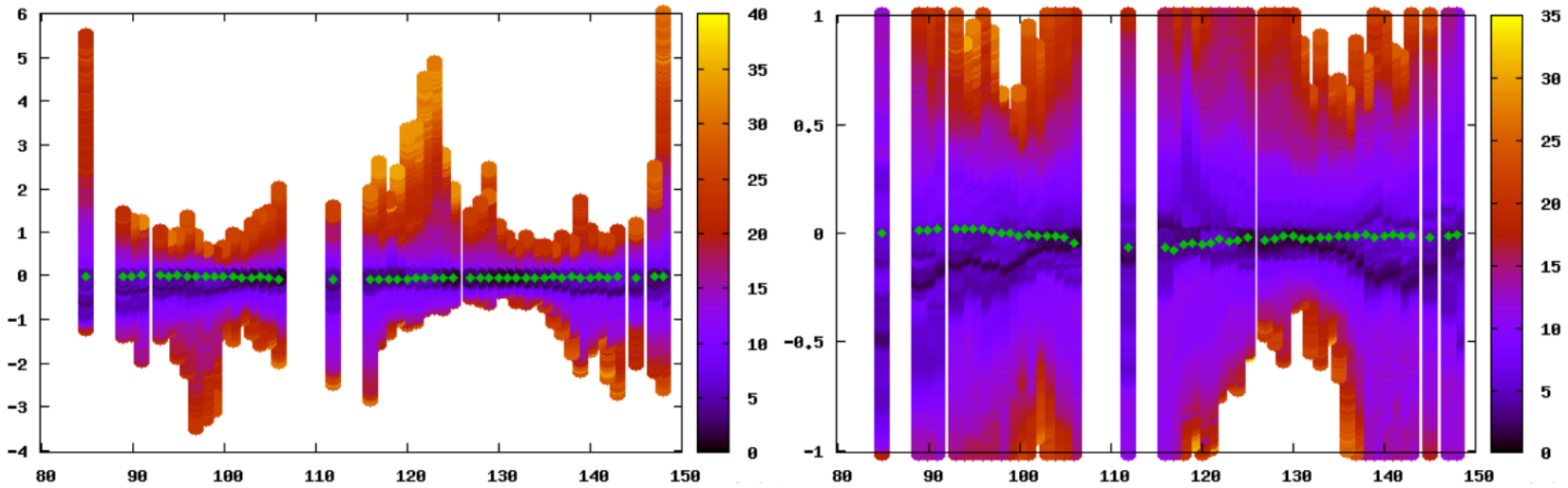

(De)Hydration reaction

$$(A \cdot 6H_2O) \underset{k_{h,a}}{\overset{k_{d,a}}{\rightleftharpoons}} (A \cdot nH_2O) + (6-n)H_2O \quad (1)$$

$$(A \cdot nH_2O) + ((B \cdot mH_2O).X)^{\ddagger} \underset{k_b}{\overset{k_a}{\rightleftharpoons}} ((A \cdot nH_2O).X)^{\ddagger} + (B \cdot mH_2O) \quad (2)$$

$$(B \cdot mH_2O) + (6-m)H_2O \underset{k_{d,b}}{\overset{k_{h,b}}{\rightleftharpoons}} (B \cdot 6H_2O) \quad (3)$$

Induced Charge Calculation

Charges in dielectric:

$$\rho^{\mathrm{i}}(\mathbf{r}) = \frac{1-\epsilon(\mathbf{r})}{\epsilon(\mathbf{r})}\rho^{\mathrm{s}}(\mathbf{r}) - \frac{\nabla\epsilon(\mathbf{r})}{\epsilon(\mathbf{r})} \cdot \epsilon_0 \mathbf{E}(\mathbf{r})$$

$$\rho^{\mathrm{e}}(\mathbf{r}) = \frac{\rho^{\mathrm{s}}(\mathbf{r})}{\epsilon(\mathbf{r})}.$$

Matrix equations:

$$4\pi\epsilon_0\ \mathbf{E}(\mathbf{r}) = \sum_k q_k^{\mathrm{e}} \frac{\mathbf{r}-\mathbf{r}_k}{|\mathbf{r}-\mathbf{r}_k|^3} + \int_{\mathcal{B}} \sigma^{\mathrm{i}}(\mathbf{r}') \frac{\mathbf{r}-\mathbf{r}'}{|\mathbf{r}-\mathbf{r}'|^3}\ da' + \int_{\mathcal{E}} \sigma^{\mathrm{e}}(\mathbf{r}') \frac{\mathbf{r}-\mathbf{r}'}{|\mathbf{r}-\mathbf{r}'|^3}\ da'$$

$$4\pi\epsilon_0\ V(\mathbf{r}) = \sum_k q_k^{\mathrm{e}} \frac{1}{|\mathbf{r}-\mathbf{r}_k|} + \int_{\mathcal{B}} \sigma^{\mathrm{i}}(\mathbf{r}') \frac{1}{|\mathbf{r}-\mathbf{r}'|}\ da' + \int_{\mathcal{E}} \sigma^{\mathrm{e}}(\mathbf{r}') \frac{1}{|\mathbf{r}-\mathbf{r}'|}\ da'$$

$$\sigma^{\mathrm{i}}(\mathbf{r}) = -\frac{\Delta\epsilon(\mathbf{r})}{\bar{\epsilon}(\mathbf{r})}\,\epsilon_0\ \mathbf{n}(\mathbf{r}) \cdot \mathbf{E}(\mathbf{r})$$

All mutants

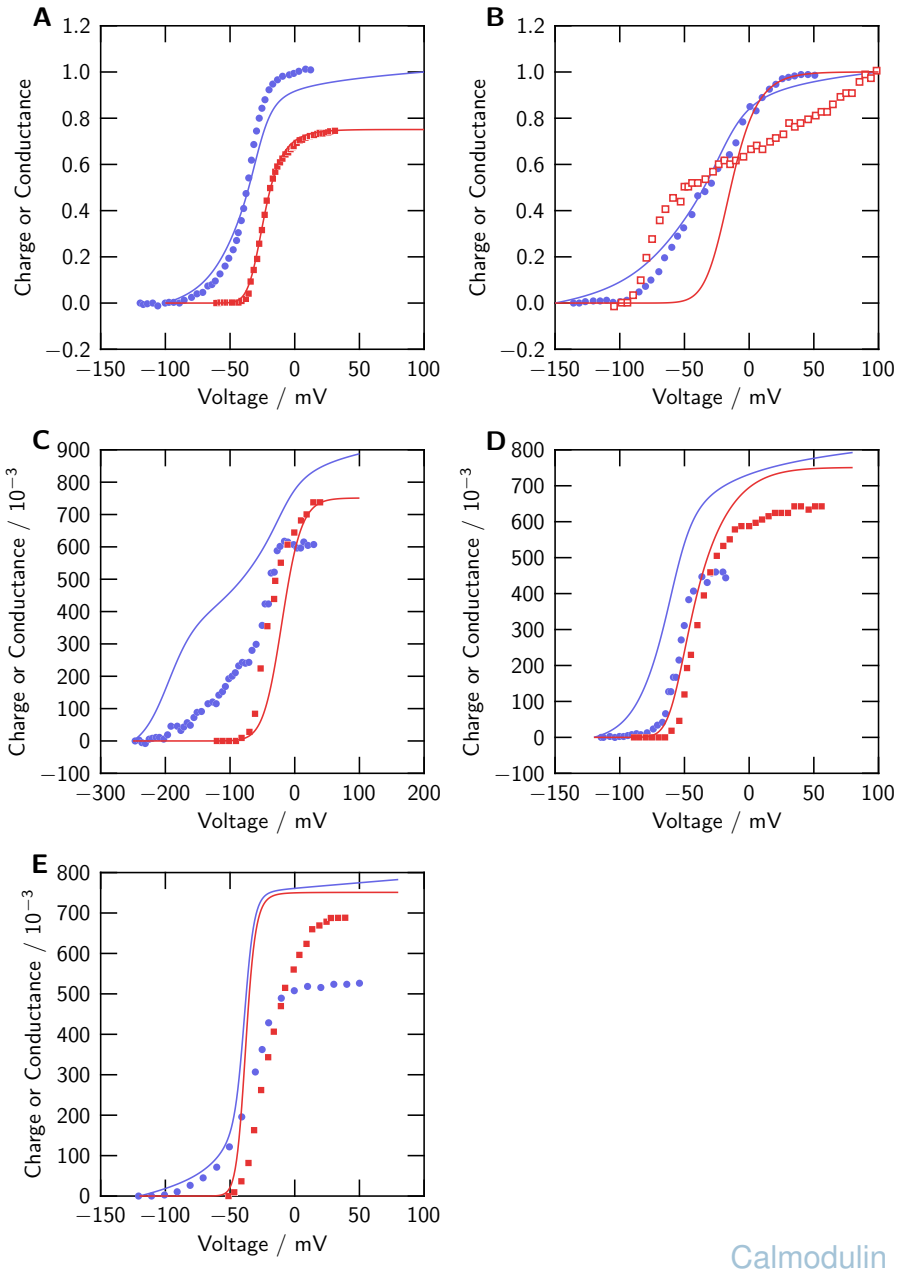
A
B
C
D
E
Charge or Conductance
Charge or Conductance / 10^{-3}
Voltage / mV

Structural plasticity

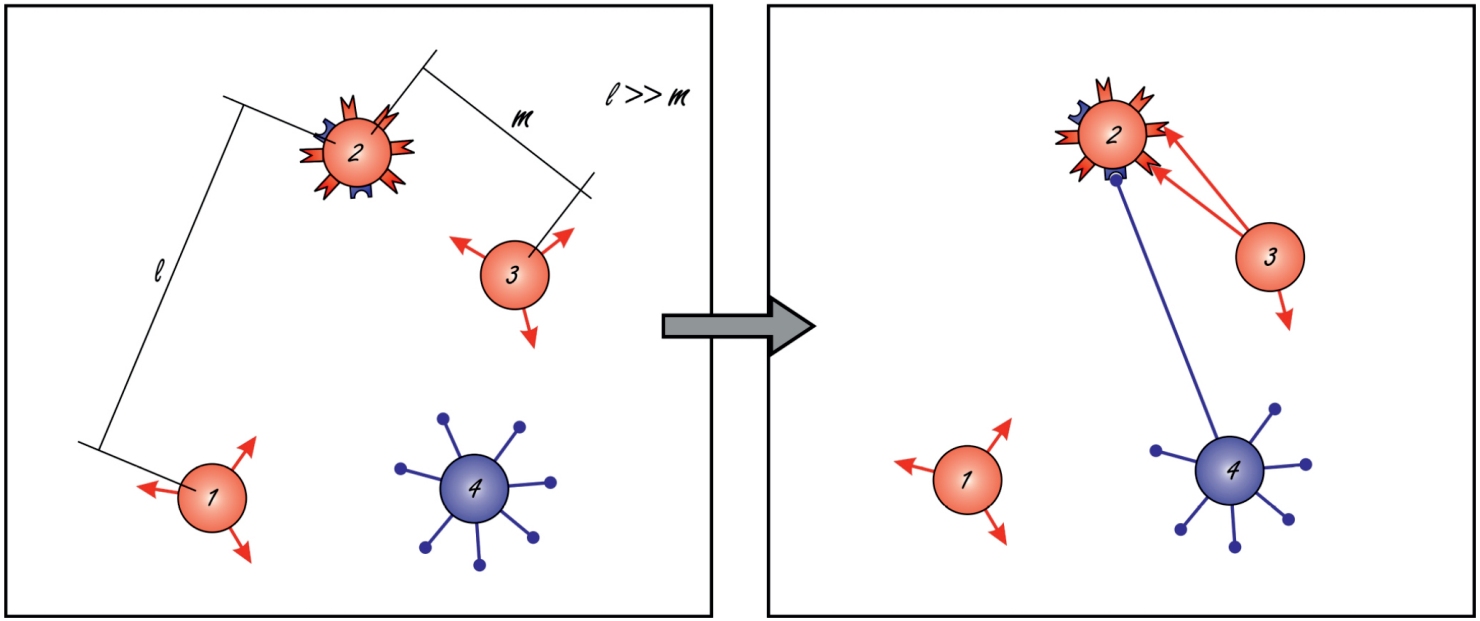

Markus Butz-Ostendorf